

---

**Resiliency Analysis of Storm Surge for Interstate 95  
Right-of-Way at Long Wharf / New Haven, CT**

Prepared by: Emmanouil Anagnostou, Ph.D.  
Wei Zhang, Ph.D., P.E.

Report Number: CT-2299-F-17-3

Final Report

March 23, 2017

Research Project: SPR-2299

University of Connecticut  
School of Engineering  
Department of Civil and Environmental Engineering

Submitted to:

Connecticut Department of Transportation  
Bureau of Policy and Planning  
Roadway Information Systems Unit  
Research Section

Michael J. Connors  
Assistant Director of Policy and Planning

## TECHNICAL REPORT DOCUMENTATION PAGE

1. Report No. CT-2299-F-17-3	2. Government Accession No. N/A	3. Recipients Catalog No.	
4. Title and Subtitle Resiliency Analysis of Storm Surge for Interstate 95 Right-of-Way at Long Wharf / New Haven, CT		5. Report Date March 23, 2017	
		6. Performing Organization Code SPR-2299	
7. Author(s) Emmanouil Anagnostou, Ph.D. Wei Zhang, Ph.D., P.E.		8. Performing Organization Report No. CT-2299-F-17-3	
9. Performing Organization Name and Address University of Connecticut Department of Civil and Environmental Engineering 261 Glenbrook Road, U-2037 Storrs, CT 06269		10. Work Unit No. (TRIS) N/A	
		11. Contract or Grant No. CT Study No. SPR-2299	
		13. Type of Report and Period Covered Final Report February 2016 to November 2016	
12. Sponsoring Agency Name and Address Connecticut Department of Transportation 2800 Berlin Turnpike Newington, CT 06131		14. Sponsoring Agency Code SPR-2299	
15. Supplementary Notes A study conducted in cooperation with the U.S. Department of Transportation, Federal Highway Administration			
16. Abstract  This report focuses on the transportation resiliency of the Long Wharf area in the City of New Haven, CT, with the aim of identifying resiliency strategies for these transportation assets. The report begins with reviewing the important transportation assets in Long Wharf area, which includes highways, bridges and railways. Subsequently, a statistical analysis is carried out to regress the extreme water levels to atmospheric forcing in the region. In order to simulate the potential total water level, a simulation scheme that combines a high-resolution atmosphere model, a land-surface model and a parametric wind-wave model is devised, considering both the actual Superstorm Sandy and simulated future scenarios. The derived total water levels from actual and future Sandy simulation scenarios are used to generate GIS-based flood inundation maps for the study area, followed by the evaluation of resiliency of the transportation assets due to flood hazards during hurricanes. Finally, based on a comprehensive review of the resiliency options utilized across US coastal regions, potential resiliency options are made for the study area.			
17. Key Words Resiliency analysis, Coasts, Floods, Infrastructure, Simulation, Storm surges		18. Distribution Statement No restrictions. This document is available to the public through the National Technical Information Service, Springfield, VA. 22161	
19. Security Classif. (Of this report) Unclassified	20. Security Classif.(Of this page) Unclassified	21. No. of Pages 50	22. Price N/A

## **DISCLAIMER**

The contents of this report reflect the views of the authors, who are responsible for the facts and accuracy of the data presented herein. The contents do not reflect the official views or policies of the State of Connecticut or the Federal Highway Administration. This report does not constitute a standard, specification or regulation.

## **ACKNOWLEDGEMENTS**

This report was prepared by the University of Connecticut, in cooperation with the Connecticut Department of Transportation and the United States Department of Transportation, Federal Highway Administration. This publication is based upon publicly supported research and is copyrighted. It may be reproduced in part or in full, but it is requested that there be customary crediting of the source. We thank Bradley Overturf, Richard Hanley, Flavia Pereira, & Michael Hogan of CTDOT and James Mahoney of Connecticut Transportation Institute for reviewing the report.



## METRIC CONVERSION FACTORS

APPROXIMATE CONVERSIONS TO SI UNITS				
SYMBOL	WHEN YOU KNOW	MULTIPLY BY	TO FIND	SYMBOL
<b>LENGTH</b>				
<b>in</b>	inches	25.4	millimeters	mm
<b>ft</b>	feet	0.305	meters	m
<b>yd</b>	yards	0.914	meters	m
<b>mi</b>	miles	1.61	kilometers	km
<b>AREA</b>				
<b>in<sup>2</sup></b>	square inches	645.2	square millimeters	mm <sup>2</sup>
<b>ft<sup>2</sup></b>	square feet	0.093	square meters	m <sup>2</sup>
<b>yd<sup>2</sup></b>	square yard	0.836	square meters	m <sup>2</sup>
<b>ac</b>	acres	0.405	hectares	ha
<b>mi<sup>2</sup></b>	square miles	2.59	square kilometers	km <sup>2</sup>
<b>VOLUME</b>				
<b>fl oz</b>	fluid ounces	29.57	milliliters	mL
<b>gal</b>	gallons	3.785	liters	L
<b>ft<sup>3</sup></b>	cubic feet	0.028	cubic meters	m <sup>3</sup>
<b>yd<sup>3</sup></b>	cubic yards	0.765	cubic meters	m <sup>3</sup>
NOTE: volumes greater than 1000 L shall be shown in m <sup>3</sup>				
<b>MASS</b>				
<b>oz</b>	ounces	28.35	grams	g
<b>lb</b>	pounds	0.454	kilograms	kg
<b>T</b>	short tons (2000 lb)	0.907	megagrams (or "metric ton")	Mg (or "t")
<b>TEMPERATURE (exact degrees)</b>				
<b>°F</b>	Fahrenheit	5 (F-32)/9 or (F-32)/1.8	Celsius	°C
<b>ILLUMINATION</b>				
<b>fc</b>	foot-candles	10.76	lux	lx
<b>fl</b>	foot-Lamberts	3.426	candela/m <sup>2</sup>	cd/m <sup>2</sup>
<b>FORCE and PRESSURE or STRESS</b>				
<b>lbf</b>	poundforce	4.45	newtons	N
<b>lbf/in<sup>2</sup></b>	poundforce per square inch	6.89	kilopascals	kPa

## TABLE OF CONTENTS

Title Page.....	i
Technical Report Documentation Page.....	ii
Disclaimer .....	iii
Acknowledgments .....	iv
Metric Conversion Factors .....	v
Table of Contents.....	vi
List of Figures.....	vii
List of Tables.....	viii
CHAPTER 1 Introduction .....	1
1.1 Description of study area .....	2
1.2 Recent flooding events .....	4
1.3 Purpose and outline .....	6
CHAPTER 2 Transportation Infrastructure in the Study Area.....	7
2.1 Interstate Highways I-91 and I-95 .....	7
2.2 Union Station and rail transportation system .....	8
2.3 Waterborne Transportation .....	8
CHAPTER 3 Statistical Analysis of Extreme Water Level .....	10
3.1 Water level data .....	11
3.2 The R largest-order statistic model .....	11
3.3 Results and discussion .....	12
CHAPTER 4 High-Resolution Atmospheric Simulations .....	14
CHAPTER 5 Parametric Wind-Wave Modeling for Hurricanes .....	15
5.1 Stochastic models for wind action .....	15
5.2 Stochastic models for wave action .....	18
5.3 Numerical results .....	21
CHAPTER 6 GIS-based flood maps .....	24
6.1 Total water level simulation .....	24
CHAPTER 7 Start-of-the-art Resiliency Options .....	29
7.1 Introduction .....	29
7.2 Resiliency options used in other U.S. coastal regions .....	30
7.3 FHWA climate resiliency pilot program .....	35
7.4 Resiliency options for Long Wharf, New Haven, CT .....	36
Concluding Remarks .....	38
Bibliography .....	39

## LIST OF FIGURES

Fig. 1.1 Storm Flooding in August 2012. ....	1
Fig. 1.2 Damage to Long Wharf Pier in New Haven, due to Superstorm Sandy .....	2
Fig. 1.3 Hurricane Irene’s Impact on Long Wharf Park.....	2
Fig. 1.4 Overview of transportation assets at I-95 Right-of-Way at Long Wharf/New Haven.....	3
Fig. 1.5 Flooded Union Avenue near Union Station in New Haven .....	5
Fig. 2.1 Pearl Harbor Memorial Bridge at I-95 .....	7
Fig. 2.2 The Port of New Haven a) Aerial view b) Google map .....	9
Fig. 3.1 Long Wharf area in the city of New Haven .....	10
Fig. 3.2 The flood inundation map during Superstorm Sandy for Long Wharf area .....	10
Fig. 3.3 Average return period in years for annual highest water levels in meters for the New Haven station.....	13
Fig. 3.4 Average return period in years for annual highest water levels in meters for the Bridgeport station .....	13
Fig. 5.1 Tracks of historical hurricanes from 1900-2015 for the study area, a circle with the city of New Haven at the center and a radius of 60 miles.....	16
Fig. 5.2 Time series and monthly distribution of hurricanes for the study area. (a) Time series; and (b) monthly distribution.....	16
Fig. 5.3 Maximum sustained 1-minute mean wind speed of the hurricanes for the study area. (a) Time series; and (b) Histogram .....	17
Fig. 5.4 Extreme 1-min sustained wind speed as a function of return period .....	18
Fig. 5.5 Flowchart of probabilistic modeling and hurricane induced wind and wave.....	21
Fig. 5.6 Simulated peak sustained wind $V_{max}$ and peak significant wave height $H_{s,c}$ corresponding to different return years .....	22
Fig. 5.7 Comparison between the wind and wave measurement from NOAA Buoy stations and the simulation results from current study .....	23
Fig. 6.1 Simulated mean wind speed for Current and Future Superstorm Sandy scenarios.....	24
Fig. 6.2 The record of water level, tide and storm surge during Superstorm Sandy 2012 .....	25
Fig. 6.3 Total water level for actual Superstorm Sandy flooding versus the simulation scenarios of future Sandy storm during low tide and high tide conditions .....	26
Fig. 6.4 Simulated flood maps for the three flooding scenarios described in Table 6.1 .....	28
Fig. 7.1 Resiliency options used in U.S. coastal regions .....	30
Fig. 7.2 2010-2011 and 2013-2015 pilot study areas. ....	36

## LIST OF TABLES

Table 3.1 Summary of NOAA station information .....	11
Table 3.2 Predicted extreme water levels corresponding to different return periods for New Haven station and Bridgeport station .....	12
Table 5.1 Modified Saffir-Simpson Hurricane Scale table .....	21
Table 5.2 Simulated peak sustained wind $V_{\max}$ , peak significant wave height $H_{s,c}$ and peak wave period $T_p$ corresponding to different return years .....	22
Table 5.3 Information on selected buoy stations in Long Island Sound .....	23
Table 6.1 Three simulated flooding scenarios .....	24
Table 6.2 Total water level flooding scenarios estimated for the different scenarios of Table 6.1 .....	26
Table 7.1 Subcategories of three main resiliency options .....	29

## CHAPTER 1 Introduction

Coastal infrastructure is extremely vulnerable to natural hazards such as hurricanes and the associated strong winds, storm surge, flooding, etc. For example, Hurricane Katrina of 2005, caused more than US \$100 billion in losses and resulted in about 2,000 fatalities with the greatest coastal flood height ever recorded in the US (Li et al. 2016). Moreover, even larger human and economic losses are expected in the future, in recognizing the steady increase in population and wealth during the past decades (Stewart et al. 2003). Recently, there has been growing evidence showing that the global climate may trigger more frequent and severe extreme events from natural hazards (Elsner et al. 2008). As reported by the Australian Greenhouse Office (2007), the peak wind speed will increase by 2–5% by the year 2030 and 5–10% by the year 2070, respectively. Knutson et al. (2010) concluded that the hurricane wind speed are likely to increase by 20% globally in the 21st century. IPCC (Intergovernmental Panel on Climate Change) also reported that both hurricane intensity and frequency may be affected due to the increase of sea surface temperature (IPCC 2007).

The city of New Haven, CT, like some other coastal communities, has been experiencing hurricane hazards more frequently in recent years. The most vulnerable areas include the Long Wharf and Morris Cove, according to *City of New Haven Natural Hazard Mitigation Plan Update* (2011). For example, Hurricane Irene in 2011 and Superstorm Sandy in 2012, which were ranked as the seventh and second costliest hurricanes in U.S., have caused catastrophic damages on the coastal communities and shorelines of Long-Island Sound, including New Haven. Due to the catastrophic Superstorm Sandy, more than 6,000 properties along the shoreline of Connecticut were subjected to various extents of damages. In particular, both hurricanes have caused severe damages to the Long Wharf area in the City of New Haven as well, e.g., the waterfront properties at Sound School were subjected to severe damages, and the Long Wharf Park and the pier sustained significant erosion. Figs. 1.1 to 1.3 show pictures of the hurricane-induced coastal flooding/damages in the Long Wharf area in New Haven, CT. However, there was no significant Connecticut Department of Transportation (CTDOT) infrastructure damages from these storms reported in this area. Due to the importance of Long Wharf area in supporting the local economy and its vulnerability to hurricane-caused flood hazards, it is necessary to perform resiliency analysis of the Long Wharf area subject to these extreme events.



**Fig. 1.1** Storm flooding in August 2012. Commuters were stranded in parking lots and other places along the shoreline including this Ikea parking lot at Long Wharf in New Haven

(Source: <http://environmentalheadlines.com/ct/2014/10/15/going-green-could-spare-flood-damage/>).



**Fig. 1.2** Damage to Long Wharf Pier in New Haven, due to Superstorm Sandy  
(Source: City of New Haven Engineering Department).



**Fig. 1.3** Hurricane Irene's Impact on Long Wharf Park  
(Source: *City of New Haven Natural Hazard Mitigation Plan Update* (2011)).

## 1.1 Description of study area

As the highway and railway gateway to New England regions, New Haven is located at the junction of Interstate 91 and Interstate 95 and serves as a key access point to the Northeast Corridor rail line (Fig. 1.4). The extensive interstate highway system (I-91 & I-95) dominates the access in and around the city and the surrounding region. Highway peak and off-peak hours often bend together. The average daily traffic could reach 129,500 vehicles per day for I-95 (City of New Haven 2015). To enhance the performance of the local transportation system, several new projects have been constructed in this area, such as the I-95 New Haven Crossing Corridor Improvement Program. The project includes reconstruction and expansion of the highway from the shoreline to Long Wharf and



includes a new Pearl Harbor Memorial Bridge and reconstruction of I-91/I-95/CT-34 interchange. Some other future expansion along Long Wharf to City Point is also planned but still in a conceptual design phase. Meanwhile, Long Wharf is a mixed use area, home to over 120 commercial buildings, key infrastructure including I-95 and the New Haven Union Station Rail yard, the CT DOT maintenance facilities and the Regional Water Authority building. The area contains key regional infrastructure built up around New Haven’s Union Station and Railway.



**Fig. 1.4** Overview of transportation assets at I-95 Right-of-Way at Long Wharf/New Haven

Due to the low elevation and exposure of this area to New Haven Harbor, flood waters have blocked access roads and underpasses for I-95 and U.S. 1, as well as portions of the rail assets in the area on several occasions during recent hurricanes or isolated thunderstorm related extreme weather events. In recognition of the importance of Long Wharf area to New Haven Harbor in supporting the local economy and its vulnerability to severe weather events, it is the necessary to perform analysis of the Long Wharf area’s resiliency to hurricane-induced flood hazards. This report aims at the vulnerability of Long Wharf area’s transportation infrastructure and develops possible resiliency strategies for these transportation assets, to mitigate the impact of future flooding events on the transportation assets located nearby.

## 1.2 Recent flooding events

In this section, we briefly discuss the damages and impacts in the Long Wharf area from two recent flood-inducing severe weather events, namely, Superstorm Sandy and Hurricane Irene. Fig. 1.5 shows the flooded Union Avenue near the Union Station.

### (1) *Superstorm Sandy (October 29, 2012)*

During Superstorm Sandy, New Haven was one of the most impacted and distressed counties in CT where 1,165 single family homes were damaged. The community experienced extensive flooding from the Harbor with surge ranging up to 7 feet high and as far inland as Church Street. The combination of a high storm surge coupled with a high-tide condition caused coastal waters to infiltrate a combined sewer overflow (CSO) that outfalls into New Haven Harbor during storm events. Collecting water from a 600-acre upland watershed, the backflow exceeded the capacity of the bypass located at West Water and Union Streets. The resulting backup-water flooded the Hill to Downtown community and converged with surge to exacerbate flooding within Long Wharf. The storm water flooding in the Hill to Downtown area inundated local streets including Route 34, Union Avenue, Church Street and other local streets in the community. Residents at the New Haven Public Meeting expressed the resulting difficulty and limitations to egress and evacuation in the area. Over 500 units of low income and elderly housing were damaged, including the Church Street South HUD Housing Complex. Upland areas within the watershed also experienced flooding, resulting in damages to key community assets including the City's Central Business District, New Haven's Historic Green, the City Municipal Complex, Yale University Campus South, and Yale Medical Center.







**Fig. 1.5** Flooded Union Avenue near Union Station in New Haven

A surge inundated Long Wharf from the Harbor, passed through the I-95 and Canal Dock Road underpasses, and converged with storm water to flood low-lying areas extending to the New Haven Rail Yard. Following Superstorm Sandy, 17 properties in the area were classified as affected under FEMA Individual Assistance Inspection Damage. Service was preemptively halted prior to the onset of Superstorm Sandy and cars were safely stored in higher areas of the yard, which limited the damages incurred. Inundation did lead to some damage of the station's low-lying power infrastructure.

In total, for New Haven County, Superstorm Sandy caused damages totaling over \$1.3 million to homes and infrastructure, while some unmet need remains. Much of this "cost" was covered by insurance and the federal government including \$78,142 in FEMA Individual and Household Grants, and \$1,153,681 in FEMA Public Assistance Grants. A study by the University of Connecticut Center for Economic Analysis found that following Superstorm Sandy, from November 2012 to December 2014, approximately 7,103 jobs were lost, with approximately half of these losses impacting small businesses.

*(2) Hurricane Irene (August 28, 2011)*

Hurricane Irene came ashore in Connecticut as a Tropical Storm with measured wind gusts in New Haven of over 60 mph. In the hours before the storm hit the shore, heavy winds battered the city and resulted in over 1,200 trees falling on the electrical lines, homes and cars. The storm was also responsible for flooding as Hurricane Irene's landfall in New Haven coincided with lunar high tide. New Haven saw a storm surge of 5-6 feet, which sent water spilling over sea walls and retaining walls. Many residents awoke to or returned home to flooded basements, yards, streets and in some cases damaged homes. In addition, more than 170 roads were either partially or completely blocked by trees, power lines, and other storm debris. United Illuminating, the local electric utility, reported that nearly 19,000 (33%) of New Haven households were without electricity. In summary, Hurricane Irene's passage through New Haven was shorter than expected, but it did linger long enough to knock down several hundred trees, flood several major roads and leave a quarter of homes in the city without power.

### *(3) Other flooding events*

According to National Oceanic and Atmospheric Administration (NOAA) National Climatic Data Center (NCDC), three flash floods and two severe storms were recorded in New Haven between 2005 and 2010. After the two storms in spring and summer of 2010, over thirty properties in the city applied for FEMA individual assistance. More recently, a March 2013 Nor'easter resulted in \$8,249,992 FEMA public assistance funds being granted to the city.

### **1.3 Purpose and outline**

In recognition of the vulnerability of New Haven to potential Atlantic Ocean hurricanes and associated hazards, this report aims at studying the Long Wharf area's transportation resiliency and proposing resiliency strategies for these transportation assets. In total, six tasks are assigned to fulfill the purpose.

- Task 1: Literature review and background check of transportation infrastructure (Chapter 2).
- Task 2: Statistical analysis of historical floods from coastal storms (Chapter 3).
- Task 3: High-resolution atmospheric simulation of Superstorm Sandy (Chapter 4).
- Task 4: Numerical simulation of hurricane induced wind and wave (Chapter 5).
- Task 5: Flood resiliency analysis based on GIS-based flood maps (Chapter 6).
- Task 6: Review of current state-of-the-art resiliency options (Chapter 7).

First, a literature review and background check of the transportation infrastructure in the study region, i.e., I-95, New Haven Rail Yard, and Union Station, is presented (Task 1). A statistical analysis of historical floods from coastal storms for the study region is followed (Task 2). To investigate the impact of future climate on hurricane severity and induced hazards on the infrastructures in the study region, high-resolution atmospheric simulations of Superstorm Sandy with different tracks under current and future climate scenarios are performed (Task 3). Those generated hurricane scenarios are used to simulate associated flooding from precipitation, surge and waves (Task 4), which are integrated into a GIS platform to create flood inundation maps (Task 5). These flood maps integrate different hazard levels that can be used to perform a preliminary hurricane induced flood hazard analysis for the coastal infrastructure at Long Wharf area in the city of New Haven. As a final step, after a comprehensive review of the current state-of-the-art resiliency options used for US coastal regions, possible resiliency options for Long Wharf area's transportation assets are discussed.

## CHAPTER 2 Transportation Infrastructure in the Study Area

### 2.1 Interstate Highway I-91 and I-95

The I-95 New Haven Harbor Crossing (NHHC) Corridor Improvement Program was being carried out at the Long Wharf area. This \$1.96 billion program with the new Pearl Harbor Memorial Bridge (Fig. 2.1) as its centerpiece includes multi-modal roadway and public transit improvements to reduce congestion in the New Haven area. This project also included the reconstruction of the I-95/ I-91/ Route 34 interchange, before the program came to a close in fall 2016.



**Fig. 2.1** Pearl Harbor Memorial Bridge at I-95

#### *I-91 & I-95*

According to CTDOT 2014 data, the average daily traffic (ADT) volume at I-95 on Long Wharf was 148,200. Previously, \$356 million funding has been allocated to the I-95/ I-91/ CT-34 Interchange Reconstruction project scheduled to be completed in Fall 2016. The contract mainly consists of the reconstruction of the I-95 / I-91 / CT-34 Interchange to accommodate increased capacity and improve interstate-to-interstate connections. The project includes twelve new ramps, twenty-one new or modified bridges and twenty-one retaining walls. New median barrier, drainage, signing and lighting will also be installed throughout the project. The new I-95 / I-91 / CT-34 Interchange will provide three travel lanes on I-95 in both directions with full shoulders, while eliminating left lane exit and entrance ramps to the extent possible. Once completed, all interstate-to-interstate connections will offer two lanes of travel. In addition, based on the GIS data, the elevation of most of the area at the Long Wharf is around 10 feet above NAVD88 datum (North American Vertical Datum of 1988), e.g., the elevation of the I-95 along the coastal line is between 5 feet and 10 feet and the elevation of the junction of I-91 and I-95 is around 15 feet.

#### *Pearl Harbor Memorial Bridge (Q) Bridge (I-95)*

The Pearl Harbor Memorial Bridge, more commonly referred to as the Q Bridge (the “Q” referring to “Quinnipiac”) by the local population, is an extradosed bridge that carries Interstate 95 (Connecticut Turnpike) over the mouth of the Quinnipiac River in New Haven, in the U.S. State of Connecticut. According to CTDOT 2014 data, the average daily traffic (ADT) volume on the bridge is 127,400. It encompasses approximately one mile of I-95 in New Haven spanning the Quinnipiac River. The new bridge includes five travel lanes and full shoulders in each direction and has a 100-year service life.

#### *The Tomlinson Lift Bridge*

The Tomlinson Vertical Lift Bridge carries four lanes of U.S. 1 traffic across New Haven Harbor and a single-track freight line owned by the Providence & Worcester Railroad that connects the waterfront with the Northeast Corridor line of Metro North and CSX. A sidewalk is present along the southern edge of the bridge.

## **2.2 Union Station and rail transportation system**

Since the early 1800's, New Haven has been a center for rail transportation. Historic Union Station is serviced by three distinct passenger rail carriers: Metro-North Railroad (MNR), Amtrak and Shoreline East. In addition, a fourth passenger rail service, The Hartford Line, is expected to enter service in 2018. Of these, both Amtrak and MNR primarily use overhead catenary electrical lines to power train sets, while the other rail services use primarily diesel-electric locomotives. These services provide a unique competitive advantage for New Haven, both for use by residents and for use by the business community. Reducing traffic congestion largely will be dependent on the future adequacy of the rail system and improvements to parking / connecting transit at the stations. From the elevation map based on the GIS data, the elevation of most of this region is less than 10 ft.

### *Amtrak*

New Haven is the busiest Amtrak station in Connecticut. New Haven is situated along two lines of service for Amtrak: the Boston- Washington "Northeast Corridor" and the New Haven – Vermont inland New England route. On the latter, New Haven serves as the terminus for Amtrak's Vermonter Line that runs to Burlington, Vermont by way of Springfield, Massachusetts. New Haven is also a stop and service point for Amtrak's Acela high-speed service, which, along with Acela Regional, complements Northeast Direct services.

### *Shoreline East*

The Shore Line East Commuter Railroad, operated by Amtrak, under contract from the State of Connecticut operates between New London and New Haven on tracks owned by Amtrak. There are seven stations on this line, several of which are undergoing renovations in association with I-95 improvements. The replacement of the Pearl Harbor Memorial Bridge may significantly enhance Shore Line East service. In anticipation of the impacts on vehicular travel, CTDOT recently opened State Street Station, which facilitates commuter movements to downtown.

### *Metro-North Railroad (MNR)*

New Haven is the northerly terminus of Metro-North Railroad's New Haven Line. The Metropolitan Transportation Authority (MTA) operates the line under a service contract and subsidy from the State of Connecticut. With 2,918 daily boardings, New Haven is the fifth busiest station along the New Haven Line. Of the New Haven boardings, 45% are at peak hour and 55% are at off-peak hours. For the line as a whole, 66% of all boardings are peak-hour.

### *New Haven Rail Yard*

CTDOT is revitalizing and expanding the existing New Haven Rail Yard (NHRY) into a state-of-the-art, coordinated facility that provides efficient and effective storage, dispatching, inspection, maintenance, and cleaning of rail cars. Located on approximately 74 acres of state-owned land that comprises the existing NHRY site, the Facilities Improvement Program is being undertaken as multiple construction projects. Facilities improvements will provide the space, equipment, and administrative support needed to operate and maintain a new generation of rail cars and will coordinate new facilities with existing facilities. CTDOT's program of improvements to the NHRY will support rail transit services in the state of Connecticut well into the twenty-first century.

## **2.3 Waterborne Transportation**

The Port of New Haven is the largest in the state in terms of volume shipped. The Port of New Haven is strategically located at the junction of Interstates 95 and 91 with access to freight rail service for the movement of cargo. The 366 acre port district is primarily comprised of a cluster of



privately owned facilities that handle petroleum products, general bulk, cargo, scrap metal, metallic products, cement, sand, stone, salt, break bulk and project cargo. In addition, there are four yacht clubs located on the coastal line of the New Haven Harbor and two out of them, Pequonnock Yacht Club and City Point Yacht Club, are located in the immediate vicinity of the Long Wharf area.

New Haven Harbor is a major commercial harbor in Connecticut and its entrance is sheltered by three breakwaters that stretch across the outer harbor in a roughly diagonal shape. These three breakwaters are comprised of the east breakwater on the east side of the channel that is 3,450 feet long, the middle breakwater parallel to the west coast line that is 4,450 feet long and the west breakwater on the west side of the channel, which is 4,200 feet long. Repairs of these three breakwaters, which were damaged during Superstorm Sandy, were performed in 2014 to restore them to the originally authorized profiles and dimensions.

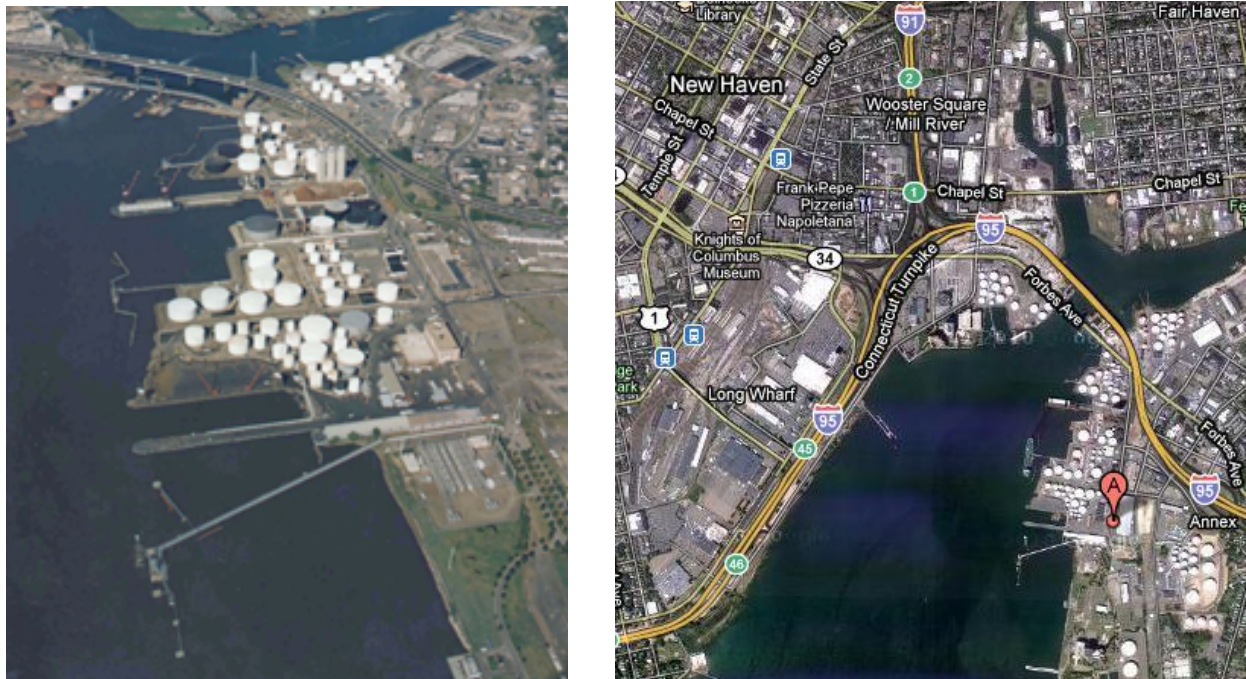


**Fig. 2.2** The Port of New Haven a) Aerial view b) Google map

### CHAPTER 3 Statistical Analysis of Extreme Water Level

During storm events, wind waves together with precipitation, cause surface runoff and surge that combined with high tides may cause flooding in shallow coastal areas. Because of the non-linear effects in the shallow coastal area, the wind waves, Mean-Sea-Level (MSL), tides and the surges are interacting with each other dynamically, which indicates the resultant total water level may be substantially different from that by a simply linear combination without considering the coupling effects. However, the interactions between wind waves, MSL, tides and the surges are quite complex and still not fully understood, although there has been a lot of research effort regarding the coupling effects (Wolf 2009). In recognizing this, we consider that the linear assumption is reasonable as it enables overall prediction of the trend of total water level and the associated impact on the low-lying coastal areas. Therefore, the present study predicted the total water level in the Long Wharf area in city of New Haven, CT as a linear combination of wind waves, MSL, tides and the surges, and precipitation-flooding effects, where each of the four components are characterized by their distinct generating mechanisms.

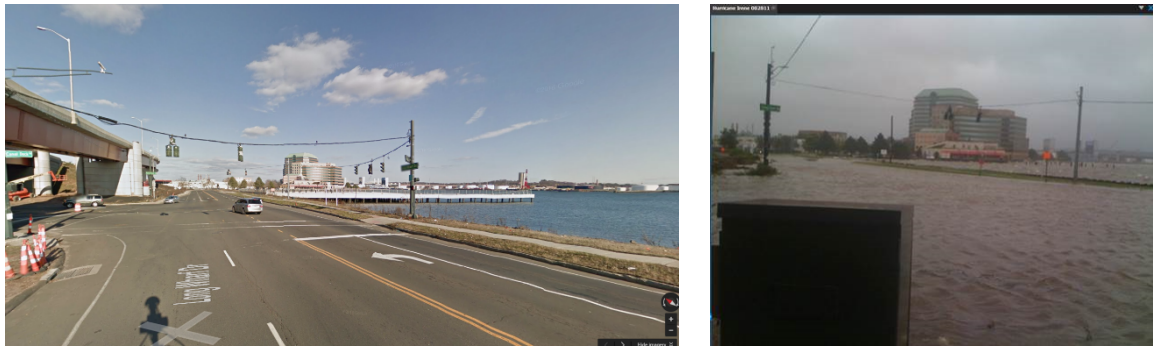


Fig. 3.1 Long Wharf area in the city of New Haven



Fig. 3.2 The flood inundation map during Superstorm Sandy for Long Wharf area

As shown in Fig. 3.1, the Long Wharf area in the City of New Haven is a low-lying coastal area, which is susceptible to heavy rainfall, storm surge, high wind and inland flooding. The structures near Long Wharf area, therefore, could be flooded due to the high water levels during these major storm events. In recognizing the steady increase in population, local economy and public facilities (e.g., Union Station and schools) in Long Wharf area (Fig. 3.2), there could be potentially even larger infrastructure and economic losses during future severe storm events.

In this section, the time series of historical water levels are examined by means of extreme value techniques. The limiting joint Generalized Extreme Value (GEV) distribution for the R largest-order statistic model is adopted to estimate return values of water levels from two NOAA stations that are near the study area.

### 3.1 Water level data

The data utilized in this study is the historical hourly water levels recorded by water level gauges. The water level data was obtained from the National Water Level Observation Network (NWLON), which is collected and maintained by the Center for Operational Oceanographic Products and Services (CO-OPS), a part of NOAA’s National Ocean Service (NOS). Many of these NWLON stations have been in operation for several decades with some having data for over a century. In the present study, the water level data from two stations, the New Haven station and the Bridgeport station, are used for analysis. The New Haven station is within 0.5 miles radius from the Long Wharf area, while the Bridgeport station is approximately 16 miles southwest of Long Wharf area. Table 3.1 summarizes the general characteristics of these two NOAA stations including the latitude and longitude, NOAA site identifier and duration of measurement. In the present study, the elevation datum for the water level data is Mean Lower Low Water (MLLW), unless otherwise noted. Also, the water level data refers to the total water level that includes the contributions from MSL, tides and the surges and no direct wave characteristics (e.g., significant wave height and peak frequency) is available for the station currently. The wave prediction for the study region is discussed in the next section.

**Table 3.1** Summary of NOAA station information

Site	NOAA ID	Latitude	Longitude	During (Year)
New Haven, CT	8465705	41.283°N	72.908°W	2001-2016
Bridgeport, CT	8467150	41.174°N	73.181°W	1970-2016

### 3.2 The R largest-order statistic model

In the present study, the extreme values theory is used to analyze the historical record of water levels. Several methods are available for the extreme value analysis in coastal engineering such as Annual Maxima method (AM), Peak Over Threshold (POT) method (Davison and Smith 1990), or R Largest Order Statistics (R-LOS) (Guedes Soares and Scotto 2004). Among those methods, the AM method can avoid the correlation among successive data, which has often been used to fit the annual maximum data by means of some extreme value distributions [e.g., (Carter and Challenor 1981; Guedes Soares and Scotto 2001)].

Nevertheless, in most cases, the extremes are scarce and the lack of enough extreme data may affect the accuracy of the model estimation significantly, i.e., the predicted extreme return levels often have large variances. To overcome this difficulty, several methods were proposed to improve the accuracy of model estimation, among which is the R-LOS method. For instance, Sobey and Orloff (1995) proposed the so called “triple annual method” to study the extremes of historical wave at the

Fallon Islands off of San Francisco, CA, from 1982 until 1992. In their analysis, the first three extreme wave height per year is used, with the purpose of reducing the statistical uncertainty among the estimators of quantiles and return years. Later, Guedes Soares and Scotto (2004) applied a similar model, the R largest-order statistic model, to estimate return values of significant wave height based on northern North Sea data set and the results indicated that this method has better performance than AM method. In this study, the R-LOS method is adopted to model the occurrences of extreme water level and to extrapolate their extreme values. The “R” in R-LOS method represents the total number of extreme events per year considered and in the present study, R=7, i.e., 7 largest measurements of the water level during each year of measurement are selected for analysis. Those identified 7 largest measurements from each year are assumed to be from independent events by requiring that time intervals among each measurement are at least 72 h.

The GEV distributions are applied to model the extreme water level, which have the following cumulative distribution function (CDF),

$$F_x(x) = \exp \left\{ - \left[ 1 + \xi \left( \frac{x - \mu}{\sigma} \right) \right]^{-1/\xi} \right\} \quad (3.1)$$

where  $x$  is a random variable, and the parameters  $\mu$ ,  $\sigma$ , and  $\xi$  control the location, scale and shape of the distribution. When  $\xi > 0$ , this distribution becomes Fréchet distribution; for  $\xi < 0$ , it is the Weibull distribution; and when  $\xi = 0$ , it becomes the Gumbel distribution. The three GEV parameters are selected to best-fit the data using a maximum likelihood approach. Based on Eq. (1), the magnitude of  $x$  corresponding to  $n$ -year return period,  $x_n$ , can be determined by solving the following equation,

$$F_x(x_n) = 1 - 1/(R \cdot n) \quad (3.2)$$

where  $R=7$  is the number of extreme values recorded per year and  $n$  is the  $n$ -year return period considered in the analysis.

### 3.3 Results and discussion

**Table 3.2** Predicted extreme water levels corresponding to different return periods for New Haven station and Bridgeport station (95% confidence intervals in parenthesis)

Return period (year)	New Haven: predicted annual extreme water level (m)	Bridgeport: predicted annual extreme water level (m)
5	3.08 (2.89, 3.36)	3.22 (3.09, 3.39)
10	3.21 (2.96, 3.60)	3.36 (3.18, 3.61)
20	3.34 (3.02, 3.88)	3.52 (3.28, 3.86)
30	3.42 (3.06, 4.07)	3.62 (3.34, 4.04)
40	3.48 (3.08, 4.21)	3.69 (3.38, 4.16)
50	3.53 (3.10, 4.33)	3.76 (3.42, 4.28)
75	3.62 (3.13, 4.55)	3.87 (3.48, 4.49)
100	3.68 (3.16, 4.73)	3.96 (3.53, 4.66)
150	3.78 (3.19, 5.00)	4.09 (3.59, 4.91)
200	3.85 (3.22, 5.20)	4.19 (3.64, 5.10)

Figs. 3.3 and 3.4 show the return period for the annual highest water levels for the New Haven station and Bridgeport station, respectively. For model validation, the measured annual extreme water levels for these two stations are also included in Figs. 3.3 and 3.4, and the results show that the proposed model can predict the annual extreme water levels reasonably well. In addition, the



point estimates corresponding to various return years for both stations are summarized in Table 3.2. It is observed from table 3.2 that on average, the predicted annual extreme water level in New Haven station is slightly (about 7%) lower than that of Bridgeport, indicating the spatial variation of extreme water levels for these two stations (about 16 miles apart) is not significant. It also shows that, based on the data corresponding to 95% confidence level, the standard error for New Haven station is larger (about 30%) than that of Bridgeport station. The reason is the relatively limited data points (i.e., 2001~2016) for New Haven station during the extreme value analysis, compared to that for the Bridgeport station (i.e., 1970~2016).

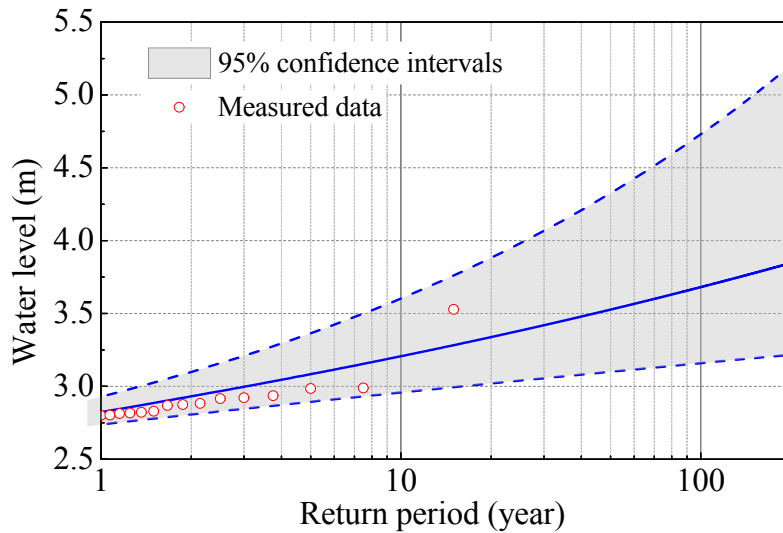


**Fig. 3.3** Average return period in years for annual highest water levels in meters for the New Haven station. Shaded envelopes and dashed lines around the solid return level curves are the GEV exceedance probabilities with 95% confidence intervals. Symbols are the measured annual maximum data. (The three GEV model parameters are:  $\mu = 2.5792$ ,  $\sigma = 0.1182$  and  $\zeta = 0.1021$ )

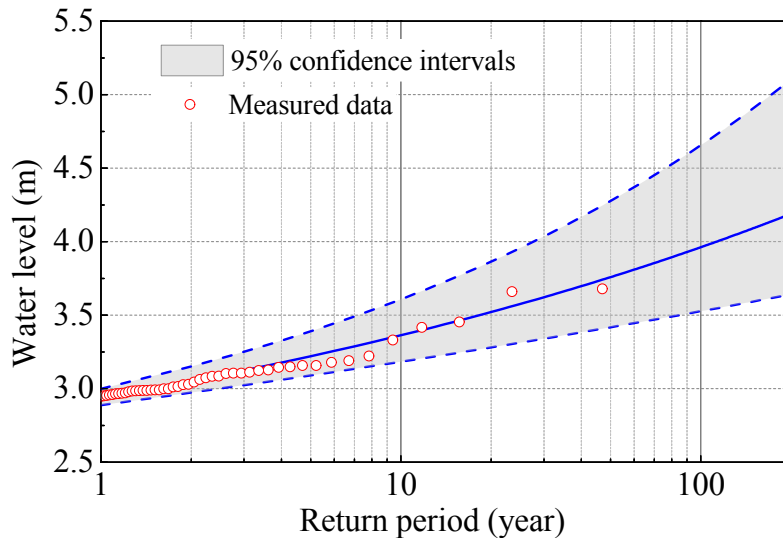


**Fig. 3.4** Average return period in years for annual highest water levels in meters for the Bridgeport station. Shaded envelopes and dashed lines around the solid return level curves are the GEV exceedance probabilities with 95% confidence intervals. Symbols are the measured annual maximum data. (The three GEV model parameters are:  $\mu = 2.7007$ ,  $\sigma = 0.1093$  and  $\zeta = 0.1591$ )

## **CHAPTER 4 High-Resolution Atmospheric Simulations**

The high-resolution atmospheric simulations were done by the Weather Research and Forecasting model (WRF) (Skamarock, W. C. et al. 2008). The details of the WRF simulations were reported in Lackmann (2015). Two different five-member ensemble simulation sets of Superstorm Sandy were used; one for the current atmospheric and oceanic conditions and the second for the future climate scenario. The model simulations included three gridded domains with 54, 18 and 6 km horizontal grid spacing using one-way nesting for the two inner grids. From the 17 members described by Lackmann (2015), five were selected to supply the wave and flooding models' input. The WRF members were selected based on the availability of the 6km domain and the variations in the physical parameterization schemes. In brief, the variations include cumulus parameterization, microphysics, and planetary boundary layer schemes. A summary of the variations in the physical parameterizations for each WRF ensemble member is provided in Lackmann (2015).

The initial and boundary conditions for the current Sandy ensemble set were obtained from the European Center for Medium Range Weather Forecasting (ECMWF) interim reanalysis (Dee et al. 2011), with an approximate spatial grid of 0.7 deg. The future Superstorm Sandy projections were based on the climatic projections from the CMIP3 project (Meehl et al. 2007). Future simulations of Sandy are produced by modifying the model initial conditions to account for General Circulation Model (GCM)-projected late-century thermodynamic changes derived from the IPCC AR4 A2 emissions scenario. More details on the modeling procedures are described in Lackmann (2015).

## CHAPTER 5 Parametric Wind-Wave Modeling for Hurricanes

There has been extensive research efforts on predicting wave characteristics (i.e., significant wave height and wave period) and investigating the impact of waves on offshore and onshore structures such as oil platform, ships, low-rise buildings, coastal bridges. In principle, the prediction of wave characteristics can be from measurement/observations, simple empirical model, or more sophisticated numerical model. The latter two approaches are developed based on the first approach, i.e., any numerical model are developed based on reliable historical data. The United States NOAA National Data Buoy Center (NDBC) network gives the global coverage of wave data (<http://www.ndbc.noaa.gov/>). Although much effort has been made on establishing the wave observation network, the number of wave buoys cannot cover all the area due to budget constraint or other limitations. In such cases, as an alternative, numerical simulation approach enables the wave prediction through numerical models that are developed mainly based on the historical data. Since wind is one of the major driving forces for waves, many methods were proposed, ranging from simple formulae for estimating wave field at a given site by using wind speed, fetch, and duration, to numerical models for wave field simulation covering large sea areas based on the input wind field time histories. Some sophisticated numerical wave prediction models, such as SWAN, WAM, WAVEWATCH models, were developed and have been widely used in various applications of weather prediction and ocean dynamics in the past few decades (Thomas and Dwarakish 2015). To simulate wind and waves for structural analysis that need higher spatiotemporal scales, spectrum and probabilistic based methods were also used (Bouws et. al. 1985, Zhu and Zhang 2017).

In this section, a probabilistic model is proposed to predict the hurricane events (e.g., hurricane frequency and intensity) and the associated sea states (e.g., wave height and period) by examining the historical hurricanes. This probabilistic model is based on parametric equations that dependent on a few key parameters, e.g., maximum wind speed, pressure deficit and translation speed, for a hurricane passing by a location. This model is straightforward and easy to use.

### 5.1 Stochastic models for wind action

#### *Hurricane data*

Fig. 5.1 shows the tracks of all historical hurricanes from 1900-2015, that affected the study area in this report. It is a circle with the city of New Haven, at the center and a radius of 60 miles around the city. There were a total of 30 hurricanes impacting the study region. The historical hurricane information obtained from US National Hurricane Center's (NHC) database (<http://coast.noaa.gov/hurricanes/>) was used to estimate the "current" characteristics of hurricanes affecting the region.

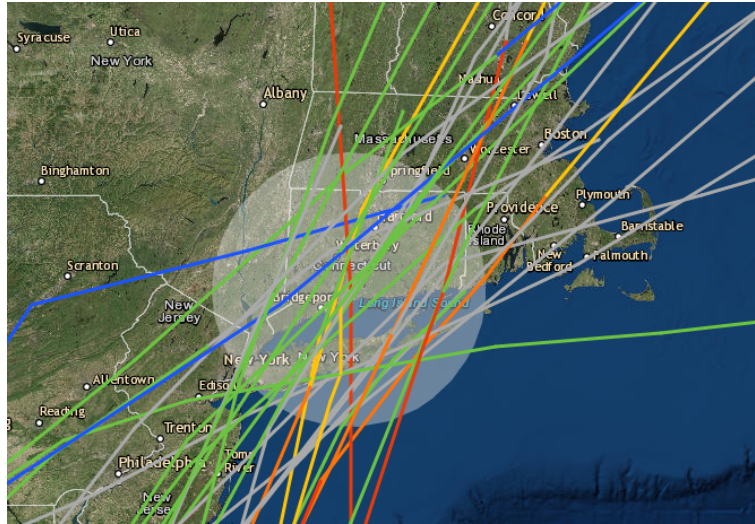


**Fig. 5.1** Tracks of historical hurricanes from 1900-2015 for the study area, a circle with the city of New Haven at the center and a radius of 60 miles (Figure reproduced from US National Hurricane Center website)

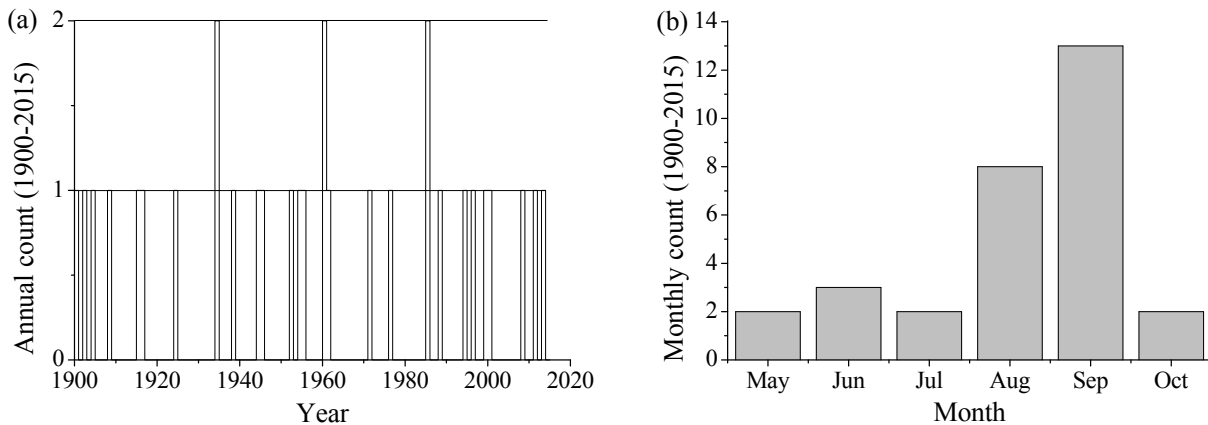


**Fig. 5.2** Time series and monthly distribution of hurricanes for the study area; **(a)** Time series; and **(b)** monthly distribution

The time series and monthly distribution of the 30 hurricanes over the 116-year period are shown in Fig. 5.2. In total, there were 89 years in which no hurricanes stroke the County in a given year, and 3 years in each of which 2 hurricanes occurred. The average annual number of hurricanes in the study region is 0.26. The hurricane season runs from the beginning of May through the end of October, and the most active months are August and September, which account for 70% of all hurricanes that stroke the study region.

Fig. 5.3 shows the time series and histogram of the maximum sustained surface wind speeds, i.e., 1-minute mean wind speed at 10 m height, of the hurricanes in the study region. Fig. 5.3 shows that 2 major hurricanes with wind speed larger than 50 m/s occurred in August and September. Given the limited hurricane data, Fig. 5.3 (a) also indicates that there seems to be no apparent long-term trend in the maximum wind speed. The mean and standard deviation of the recorded wind speed are 26.43 m/s and 11.00 m/s, respectively. Fig. 5.3 also shows that the maximum historical wind speed in New Haven is 54 m/s, which corresponds to a Category-3 hurricane. This finding is consistent with ASCE 7-10 (2013), indicating that the Category-3 hurricane could be the possible worst hurricanes that can strike the City of New Haven.

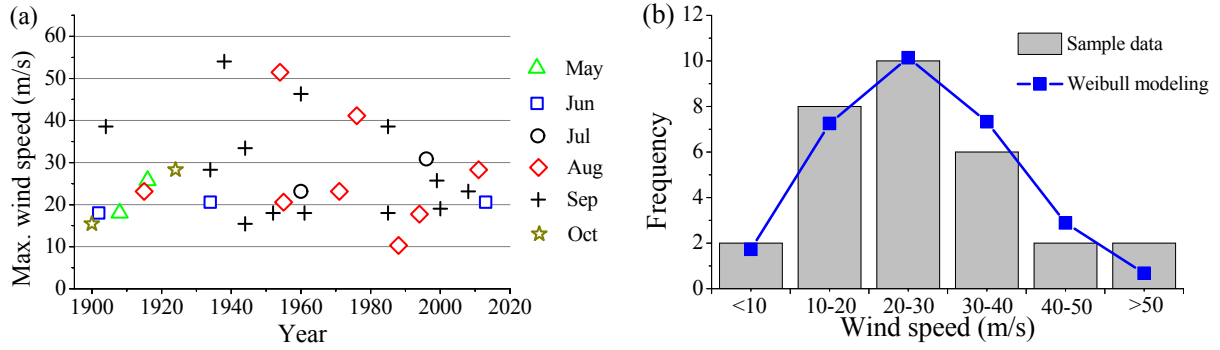


**Fig. 5.3** Maximum sustained 1-minute mean wind speed of the hurricanes for the study area. **(a)** Time series; and **(b)** Histogram

### Stationary wind process

In the proposed study, the storm occurrence is modeled as a Poisson point process (Li et al. 2016), in which the probability that  $n$  storms occur within a time interval  $(0, T]$  is given by,

$$\Pr(N_T = n) = \frac{(\lambda T)^n \exp(-\lambda T)}{n!} \quad (n=0,1,2,\dots) \quad (5.1)$$

where  $\Pr()$  is the probability of the event in the bracket; and  $\lambda$  is the mean occurrence rate of the storms, which is assumed to be constant for a stationary hurricane storm process.

Although Weibull distribution has often been used to model the annual extreme wind speed (Batts et al. 1980; Peterka and Shahid 1998), it's use is questionable as there is a finite probability that the hurricane wind speed is zero (i.e., hurricane does not occur). In some researches, the GEV distributions is adopted to model the annual extreme wind speed (Valamanesh et al. 2015). In the present study, instead of using the concept of annual extreme hurricane wind speed, the Weibull distribution is used to model the probability distribution of the maximum wind speed during a hurricane event. The cumulative density function (CDF) of the hurricane wind speed described by the Weibull distribution is given by,

$$F_v(v) = 1 - \exp\left[-\left(\frac{v}{u}\right)^\alpha\right] \quad (5.2)$$

where  $v$  is the 1-min sustained wind speed,  $u$  and  $\alpha$  are two site-specific parameters for the Weibull distribution that are estimated by the recorded historical hurricane wind speed data.

The two Weibull parameters are found to be  $u=29.84$  m/s and  $\alpha=2.58$ , based on the Weibull fit to the recorded historical hurricane wind speed data of the study area. Fig. 5.3 (b) shows a comparison between the frequency from the actual wind speed data and that derived from the fitted Weibull distribution and the result confirms that the Weibull distribution is an appropriate and reasonable model for the hurricane wind speed. The parameters for both the Poisson model and Weibull model are assumed to be constant, if no effects of climate change are considered.

The wind speed exceedance probability during a time period  $(0, T]$  can then be expressed by Weibull wind speed that is conditioned on the Poisson hurricane occurrence as,

$$\Pr(V > v) = 1 - \sum_{i=0}^{\infty} \Pr(V < v | N_T = i) \cdot \Pr(N_T = i) \quad (5.3)$$

where  $\Pr(V < v | N_T = i)$  is the conditional probability that wind speed is less than  $v$  given that  $i$ th hurricane occur which is described by Weibull distribution, and  $\Pr(N_T = i)$  is the probability of  $i$ th hurricane during the time period  $(0, T]$  which is described the Poisson process. Accordingly, the CDF of the extreme wind speed during the time period  $(0, T]$  can be expressed as,

$$F_T(v) = \exp[-\lambda T(1 - F_v(v))] \quad (5.4)$$

With parameters for the Weibull distribution and Poisson process estimated from the recorded data in the study area, i.e.,  $\lambda=0.259/\text{year}$ ,  $u=29.84$  m/s and  $\alpha=2.58$ , the extreme sustained 1-min wind speed with respect to different return years are obtained from Eq. 5.4. To illustrate the proposed model, Fig. 5.4 compares the results of current study with the wind speed map from ASCE 7-10 (2013) for the study region. Note that the wind speed map of ASCE 7-10 is 3-s gust wind speed and is converted to 1-min sustained wind speed before the comparison by applying a scale factor of 0.82. Fig. 5.4 shows that the extreme wind speeds estimated by the current study are about 10% larger than those from the ASCE 7-10. This discrepancy is due to different methods used for predicting the extreme wind speed. The proposed study is based on statistical analysis of very limited historical hurricane data using straightforward and simple model, while the ASCE 7-10 is based on the simulation of thousands years of hurricane events utilizing more sophisticated and complicated model (e.g., empirical track model, central pressure model, etc.) (Vickery et al. 2000).

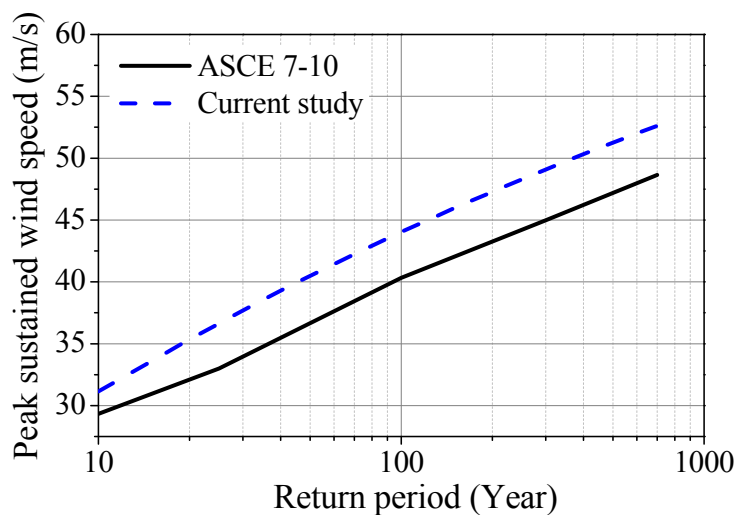


**Fig. 5.4** Extreme 1-min sustained wind speed as a function of return period

## 5.2 Stochastic models for wave action

### *Empirical model for hurricane induced wave*

Some sophisticated numerical wind and wave prediction models, such as ADCIRC, SWAN, WAM, WAVEWATCH models, have been developed for hurricane-induced wind and wave prediction (Thomas and Dwarakish 2015). However, these models are computationally demanding and due to their large spatiotemporal scales, the resolutions for the simulated wind and waves are low, which may either underestimate or overestimate the site-specific wind and wave conditions. As an alternative, empirical models have been proposed to predict the hurricane induced wind and waves. Although many of these models are for predicting the wind speed given hurricane characteristics (e.g., Li et al. 2016b; Vickery et al. 2000), few are concerning the prediction of hurricane-induced waves.

Young (1988a, 2003) proposed an empirical model to predict the spatial distribution of the

significant wave height  $H_s$ , during hurricanes based on three hurricane parameters, i.e., the radius to maximum winds  $R_{max}$ , the maximum wind speed  $V_{max}$ , and the translation speed  $V_{tr}$ . Young's model introduces the concept of equivalent fetch length to account for the situation where the wave speed is comparable to the translation speed of hurricane, so that the JONSWAP fetch-limited growth relationship still holds under hurricane conditions. Their underlying assumption is that the energy can be transferred from wind to the waves over an effectively longer length, which is represented through an extended fetch or trapped fetch (Young and Vinoth 2013). With the specification of an extended, equivalent fetch length, the significant wave height and peak frequency can then be determined by the modified JONSWAP relationship. The significant wave height,  $H_s$ , by conventional definition is the average of the top one third of recorded wave height in a given time interval and the peak spectral frequency,  $f_p$ , is defined as the frequency of sea state corresponding to the greatest power spectral density. Based on the comprehensive synthetic model and in situ measurement databases, Young and Vinoth (2013) proposed a parametric model for equivalent fetch,  $F$ , for tropical cyclones,

$$F = R' \varphi (a_1 V_{max}^2 + a_2 V_{max} V_{tr} + a_3 V_{tr}^2 + a_4 V_{max} + a_5 V_{tr} + a_6) \quad (5.5)$$

where  $a_1 \sim a_6$  are coefficients given by  $a_1 = -2.175 \times 10^{-3}$ ,  $a_2 = 1.506 \times 10^{-2}$ ,  $a_3 = -0.122$ ,  $a_4 = 8.760 \times 10^{-2}$ ,  $a_5 = 1.516$  and  $a_6 = 1.756$ ;  $\varphi = -0.015 V_{max} + 0.0431 V_{tr} + 1.30$  is dimensionless scaling factor; and  $R' = 22500 \log R_{max} - 70800$  is the effective radius to maximum winds. Note that all values are in standard S.I. units unless noted otherwise.

The maximum significant wave height,  $H_s^{max}$ , can be determined using JONSWAP fetch limited growth relationship (Hasselmann et al. 1973),

$$\frac{g H_s^{max}}{V_{max}^2} = 0.0016 \left( \frac{g F}{V_{max}^2} \right)^{0.5} \quad (5.6)$$

where  $g$  is the gravitational acceleration. Note that Eq. (5.6) only gives the estimation of maximum significant wave height. The spatial distribution of significant wave  $H_s$  within a storm is scaled from  $H_s^{max}$  through a series of non-dimensional spatial distribution diagrams.

From Eq. (5.5), the radius to maximum wind  $R_{max}$  is required to calculate the equivalent fetch. Due to the lack of data in the study region, the radius to maximum wind  $R_{max}$  (in km) can be approximated formulated in terms of central pressure deficit  $\Delta p$  (in mbar) and the latitude  $\psi$  (in degree) as (Vickery et al. 2000),

$$\ln R_{max} = 2.097 + 0.0187793 \Delta p - 0.00018672 \Delta p^2 + 0.0381328 \psi \quad (5.7)$$

Note that Young's model was developed for estimating the wave characteristics under deep water conditions in the open ocean where the seafloor does not affect the waves. However, for the offshore structures that are generally located in shallow water, both the land and seafloor may have significant influence on waves, indicating the necessity to include the shallow water effect for better estimation of significant wave height and peak frequency. Valamanesh et al. (2016) pointed out that Young's model tends to overestimate the significant wave height in shallow water and proposed a bias-corrected equation to account for the effects of water depth, based on the measured hurricane wave data from 22 offshore buoys located along the US Atlantic and Gulf of Mexico coasts. The equation assumes that the corrected maximum significant wave height  $H_{s,c}^{max}$ , is calculated in terms of water depth  $d$  and the corresponding maximum significant wave height  $H_s$ ,

$$\ln(H_{s,c}^{\max}) = -e^{0.06d} + \ln(H_s^{\max}) \quad (5.8)$$

Based on the study of hurricane induced directional wave spectra using in situ data, Hu and Chen (2011) and Young (2006) found that the wave spectra within the storm generally conform to the standard JONSWAP form. These observations may also explain that the proposed JONSWAP scaling (Eq. 5.6) is capable of predicting the significant wave field reasonably well. As suggested by Young (2006), the JONSWAP relationship can be expressed in terms of the non-dimensional total energy,  $\varepsilon = g^2 E / V_{\max}^4$ , and the non-dimensional peak frequency,  $\nu = f_p V_{\max} / g$ ,

$$\varepsilon = 6.365 \times 10^{-6} \nu^{-3.3} \quad (5.9)$$

where  $H_{s,c} = 4\sqrt{E}$ ,  $H_{s,c}$  is the corrected significant wave height determined from Eq. (5.8),  $E = \int F(f)df$  and  $F(f)$  is the one-dimensional variance spectrum. Therefore, the peak frequency,  $f_p$ , can be determined from the above relationships.

#### *Modified Saffir-Simpson Hurricane Scale table*

As indicated by Eqs. (5.5) ~ (5.7), in addition to the maximum wind speed that can be obtained from the stochastic wind action model discussed previously, the translation wind speed and the central pressure deficit are also needed in order to predict the hurricane induced wave height. Note that these parameters are currently not available in the database. Although it may be difficult to establish an empirical model of  $\Delta p$  and  $V_{tr}$  due to lack of recorded data for the study region, both  $\Delta p$  and  $V_{tr}$  can be characterized according to Saffir-Simpson scale (table 5.1) if a hurricane is assigned a Saffir-Simpson category.

The Saffir-Simpson Hurricane Scale is a 1-5 rating based on a hurricane's 1-min sustained wind speed, which has been most widely used by hurricane forecasters and emergency managers for categorizing hurricane intensity and estimating the potential property damage along the coast from a hurricane land fall (Simiu et al. 2007). Vickery et al. (2000) also included the central pressure in the hurricane scale to help better distinguish the hurricanes, based on the magnitude of the central pressure and sustained wind speed at the time of landfall from synthetic database of 20,000-year simulated hurricanes. Note that the wind speed (1-min sustained wind) is the determining factor in the scale and the wind speed for even the weakest hurricane (i.e., hurricane category 1) is 33-42 m/s, which means that more than half of the historical hurricanes (i.e., wind speed  $\leq 33$  m/s) in the study region is not qualified for the hurricane scale table. Therefore, in recognizing this and for better modeling the hurricane induced wind and wave, another two storm intensity categories, i.e, Tropical Depression (TD) and Tropical Storm (TS), are included in the hurricane scale table 5.1.

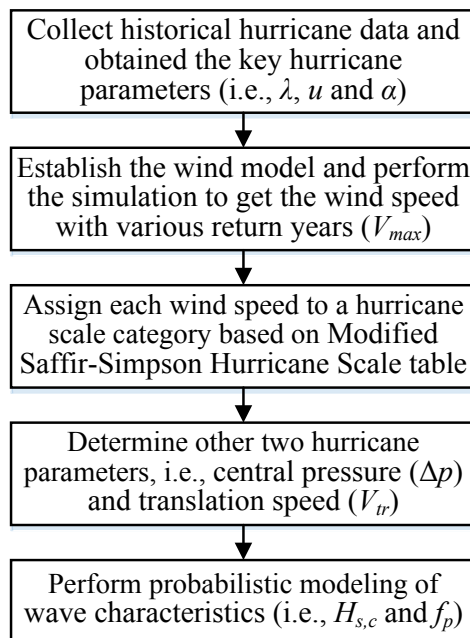
In addition, it is also possible to include the hurricane translation speed in the hurricane scale table, according to the study by Lin et al. (2008) and Mei et al. (2012). Mei et al. (2012) investigated the best-track of more than 3090 TC (Tropical Cyclone) that occurred during 1970-2010 and found that the translation speed of a storm can exert a significant control on the intensity of storms by modulating the strength of the negative effect of the storm-induced sea surface temperature (SST) reduction on the storm intensification (i.e., the SST feedback). The results also showed that the storm mean translation speed, i.e., averaged over each TC intensity category, positively correlates with TC intensity. In the present study, the averaged translation speed of mean  $\pm$  standard deviation (SD) for each TC intensity category provided by Mei et al. (2012) is included in the hurricane scale table 5.1.



**Table 5.1** Modified Saffir-Simpson Hurricane Scale table

Saffir-Simpson Category	Maximum sustained 1-min wind [m/s (mph)]	Central pressure (mbar)	Translation speed [m/s (mph)]
TD	≤17 (≤38)	980-1013	2.25-5.61 (5.03-12.55)
TS	18-32 (39-73)	980-1013	2.42-5.84 (5.41-13.06)
1	33-42 (74-95)	980-1013	2.72-6.04 (6.08-13.51)
2	43-49(96-110)	965-979	3.01-6.22 (6.73-13.91)
3	50-58 (111-129)	945-964	3.13-6.37 (7.00-14.25)
4	59-69 (130-156)	920-944	3.30-6.52 (7.38-14.58)
5	≥70 (≥157)	<920	3.57-7.31 (7.99-16.25)

Finally, the modified Saffir-Simpson Hurricane Scale is shown in table 5.1, where the storms are classified into 7 categories based on the 1-min sustained wind speed and the possible ranges of central pressure and translation speed are provided as well.

**Fig. 5.5** Flowchart of probabilistic modeling and hurricane induced wind and wave

### 5.3 Numerical results

The flowchart of the probabilistic prediction of hurricane induced wind and wave is shown in Fig. 5.5, and the corresponding procedures are summarized as follows. First, for a given study area, collect the historical hurricane data and perform the statistical analysis to obtain the key parameters such as hurricane frequency and intensity. Second, establish the stochastic wind model based on the hurricane wind speed data, through Eqs. (5.1)~(5.4). Once the wind model is established, the wind speed during hurricane events corresponding to different return year can be determined. Third, the wind speed with various return year can be assigned to a hurricane scale category based on the Modified Saffir-Simpson Hurricane Scale table (table 5.1), and the corresponding central pressure and translational speed range are determined as well. It is assumed that both the central pressure and the translational speed are uniformly distributed for the specified range of the corresponding scale category. Finally, the simulated various return year wind speed together with the uniformly distributed central pressure and translation speed are used for the wave characteristics (i.e.,  $H_{s,c}$  and  $f_p$ ).

$f_p$ ) prediction through Eqs. (5.5)~(5.8).

**Table 5.2** Simulated peak sustained wind  $V_{\max}$ , peak significant wave height  $H_{s,c}$  and peak wave period  $T_p$  corresponding to different return years

Return period (year)	1-min sustained wind $V_{\max}$ (m/s)	Significant wave height $H_s$ (m) (mean $\pm$ standard deviation)	Peak wave period $T_p$ (s) (mean $\pm$ standard deviation)
10	31.15	$3.81 \pm 0.13$	$5.76 \pm 0.29$
20	35.34	$4.37 \pm 0.15$	$6.02 \pm 0.29$
30	37.69	$4.65 \pm 0.17$	$6.10 \pm 0.30$
40	39.28	$4.83 \pm 0.18$	$6.14 \pm 0.31$
50	40.49	$4.97 \pm 0.19$	$6.18 \pm 0.32$
100	44.02	$5.54 \pm 0.19$	$6.43 \pm 0.32$
200	47.29	$5.87 \pm 0.22$	$6.47 \pm 0.34$
500	51.25	$6.24 \pm 0.25$	$6.52 \pm 0.35$
600	52.00	$6.29 \pm 0.26$	$6.51 \pm 0.36$
700	52.62	$6.34 \pm 0.27$	$6.51 \pm 0.37$
800	53.15	$6.38 \pm 0.28$	$6.50 \pm 0.37$
900	53.61	$6.41 \pm 0.28$	$6.50 \pm 0.38$
1000	54.02	$6.44 \pm 0.28$	$6.49 \pm 0.38$

The simulated peak sustained wind  $V_{\max}$ , peak significant wave height  $H_{s,c}$  and peak wave period  $T_p$  corresponding to different return years are showed in table 5.2. In addition, the simulated peak sustained wind speed and peak significant wave height corresponding to different return years are plotted in Fig. 5.6. It is shown in Fig. 5.6 that both significant wave height  $H_{s,c}$  and sustained wind  $V_{\max}$  increase almost linearly with return years (note logarithmic scale is adopted for  $x$ -axis). Fig. 5.6 also shows that the peak sustained wind speed positively correlates with peak significant wave height (the correlation coefficient is 0.99).

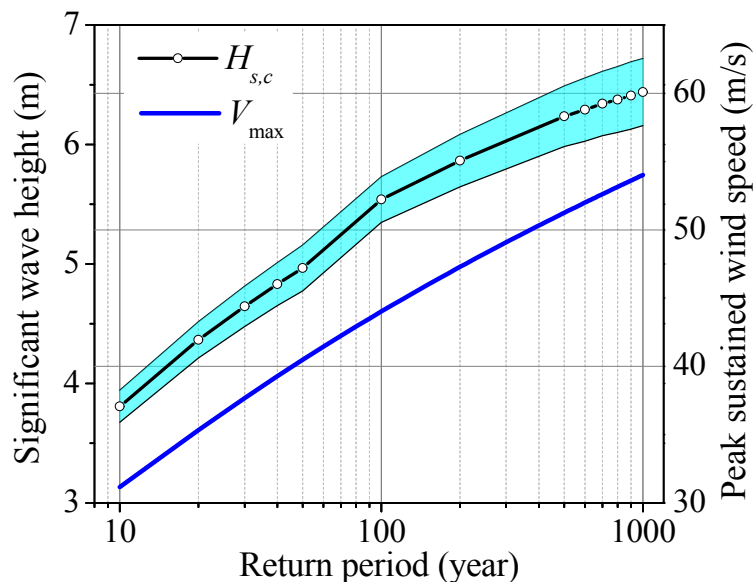


**Fig. 5.6** Simulated peak sustained wind  $V_{\max}$  and peak significant wave height  $H_{s,c}$  (the shading indicates  $\pm$  one standard deviation (SD)) corresponding to different return years

To illustrate the proposed model, Fig. 5.7 compares the simulation results with the wind and wave measurement during hurricanes that are obtained from NDBC. The two nearby buoy stations used for validation are: Central Long Island Sound Station 44039, which is approximately 14 miles southeast of New Haven Harbor; and Western Long Island Sound Station 44040, which is

approximately 35 miles southwest of New Haven Harbor. Other information about these two buoy stations is summarized in table 5.3. Fig. 5.7 suggests that the bulk of data are concentrated in the lower region, i.e.,  $V_{\max} \leq 25$  m/s and  $H_{s,c} \leq 3$  m, possibly due to the relatively short time period of measurement data collection (from 2004~2015). This may also indicate that the Long Island Sound, including New Haven, is less likely to suffer from more severe hurricane hazards, compared with the Gulf of Mexico. Overall, the prediction model captures the trend of the maximum wind speed and significant wave height during hurricane events.

**Table 5.3** Information on selected buoy stations in Long Island Sound

Data Source	Station Name & Number	Geographical Coordinates		Time Period		Water depth (m)
		Lat. (N) [°]	Lon. (E) [°]	Start	End	
NDBC, NOAA	Central Long Island Sound Station (44039)	41.138	-72.655	2004	2015	27
NDBC, NOAA	Western Long Island Sound Station (44040)	40.956	-73.58	2006	2015	18.3

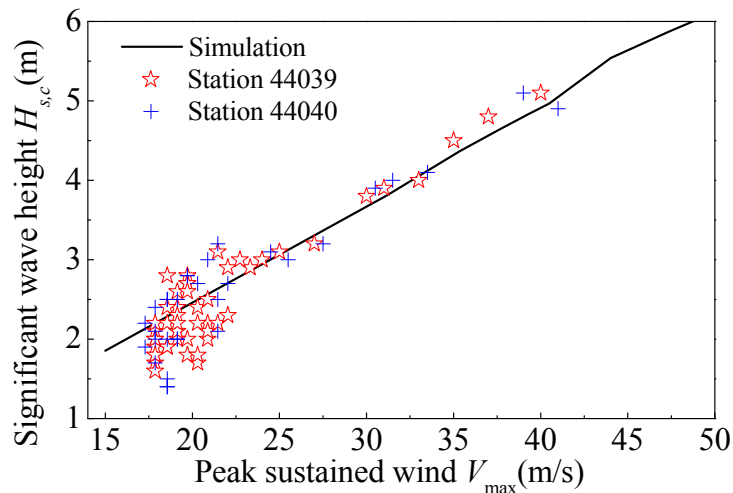


**Fig. 5.7** Comparison between the wind and wave measurement from NOAA Buoy stations and the simulation results from current study (the significant wave height is the mean value from table 5.2)

## CHAPTER 6 GIS-based flood maps

As discussed earlier, several storms including Superstorm Sandy and Hurricane Irene affected this region with severe flooding impacts. Under different storm tracking scenario, Superstorm Sandy could have caused more damage if the flooding inundation was superposed with high tides. In addition, future climate trends could bring additional threat to this low-lying region. In the present study, the total water level (TWL) is assumed as the superposition of different water level contributions including surge, wind induced waves, precipitation-induced water level, sea level rise, and tides into three different simulation scenarios. The scenarios are summarized below in Table 6.1. Scenario 1 represents the actual Superstorm Sandy scenario, which is based on historical data of flood level. In simulated Scenarios 2 and 3, the wind time histories are obtained from a high resolution atmospheric model simulation of five possible Superstorm Sandy tracks with consideration of climate conditions. The differences between Scenario 2 and 3 is that Scenario 3 considers Superstorm Sandy occurring at high tide, while Scenario 2 is at low tide.

**Table 6.1** Three simulated flooding scenarios. Scenario 1 represents actual Superstorm Sandy flood levels, while Scenarios 2 and 3 represent future climate storm Sandy simulations occurring during low and high tides, respectively.

	Surge	Wind	Wave	Inland Flooding	Sea level	Tides	Brief
1	Historical data	Historical data	Historical data	Historical data	Historical data	Historical data	Current Sandy
2	Historical data	Simulated (Chapter 4)	Simulated (Chapter 5)	Simulated (Chapter 6)	Sea level rise	Historical low tides	Future Sandy low tide
3	Historical data	Simulated (Chapter 4)	Simulated (Chapter 5)	Simulated (Chapter 6)	Sea level rise	Max tides	Future Sandy high tide

### 6.1 Total water level simulation

#### *Hurricane wind and wave*

Based on the simulation procedures discussed in section 4, the mean wind speed during future Sandy is shown in Fig. 6.1 and is compared with the historical wind speed. The historical wind speed is obtained from NOAA station in Bridgeport (see table 3.1). Fig. 6.1 indicates that overall the mean wind speed for future Sandy scenario will be about 5% more than the historical wind speed and the peak wind speed.

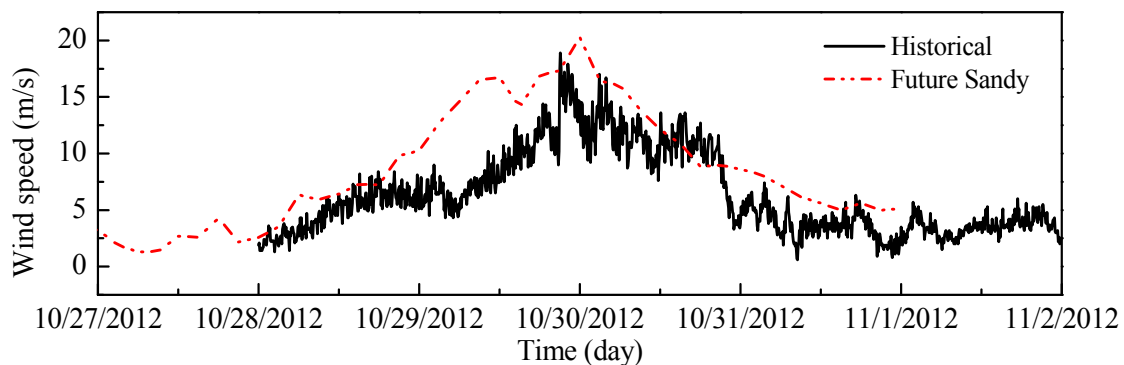


**Fig. 6.1** Simulated mean wind speed for Current and Future Sandy scenarios

### Storm surge and tide data

In addition to the wind waves, the storm surge and tide data are required to predict the total water level during Superstorm Sandy scenarios. In the present study, both the storm surge and tide data are derived based on the measurement data from the NOAA station located near New Haven Harbor (please refer to table 3.1 for details) during Superstorm Sandy. The NOAA station in New Haven has both the water level and tide data available and for simplicity, the storm surge can be assumed as the difference between the measurement water levels and the elevation of the astronomically predicted tide. Fig. 6.2 shows the time histories of storm surge, tide and water level during Superstorm Sandy 2012. In addition, the MSL is 1.012m, according to this station. In the present study, the elevation datum for the water level, tide and MSL is the MLLW, unless otherwise noted.

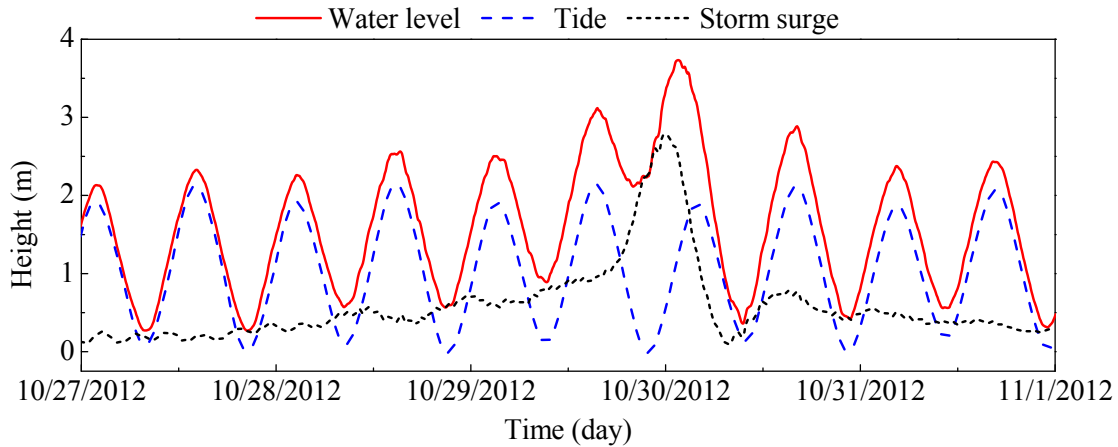


**Fig. 6.2** The record of water level, tide and storm surge during Superstorm Sandy 2012 (the elevation datum is the MLLW, unless otherwise noted). The data is obtained from NOAA station 8465705 in New Haven, CT

### Water level due to precipitation

Water level due to precipitation is obtained using the Soil-Vegetation-Atmosphere-Snow version of the Coupled Routing and Excess Storage (CREST-SVAS) hydrological model. The model is selected as the framework of this study due to its capability of running efficiently at fine spatiotemporal resolution (100-1km and hourly time scale) over long periods (a few decades) and for large basin areas ( $\sim 10^6 \text{km}^2$ ) (Shen et al. 2016). It is a physically-based runoff-generation module that explicitly represents different vegetation structures and the snow process. The runoff-generation module solves coupled water and energy balances (EB) using precipitation, meteorological variables (radiation, humidity, wind speed), and Leaf Area Index (LAI), as well as land cover, soil properties, vegetation species description and impervious ratio as static parameters. The complete form of EB in an arbitrary layer in the alto can be formulated by equation (6.1),

$$R_n = H + E - G + \Delta H + \Delta M \quad (6.1)$$

where  $R_n$  is the net radiation ( $\text{W/m}^2$ ),  $H$  is the sensible heat,  $E$  is the latent heat,  $G$  is the conductive heat flux,  $\Delta H$  is the heat storage change of the medium,  $\Delta M$  is the heat induced by mass changes.

### Total water levels (TWL) for different scenarios

Based on the previous simulated and measured data, the total water level (TWL) for the three most

severe Superstorm Sandy scenarios defined in Table 6.1 were obtained and summarized in Table 6.2.

**Table 6.2** TWL flooding scenarios estimated for the different scenarios of Table 6.1

	Maximum total water level	Time (UTC)	Description
1	3.73	10/30/2012: 00	Actual Superstorm Sandy conditions
2	4.911	10/30/2012 0:00	Surge + simulated wave + inland flooding+ sea level rise + future sandy low tides
3	6.495	10/30/2012 0:00	Surge + simulated wave + inland flooding+ sea level rise + future sandy high tides

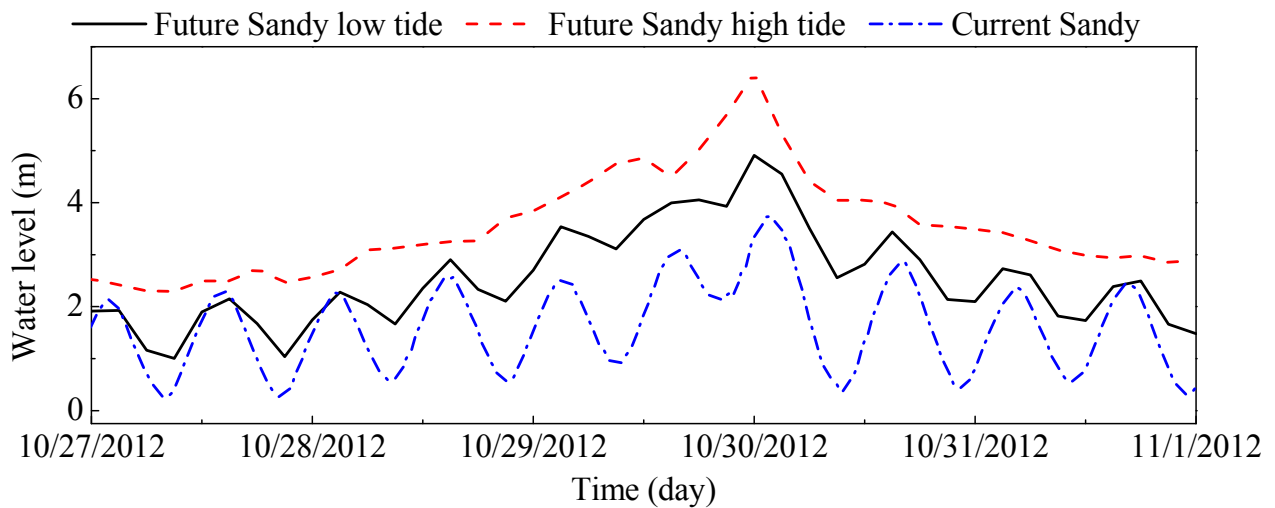
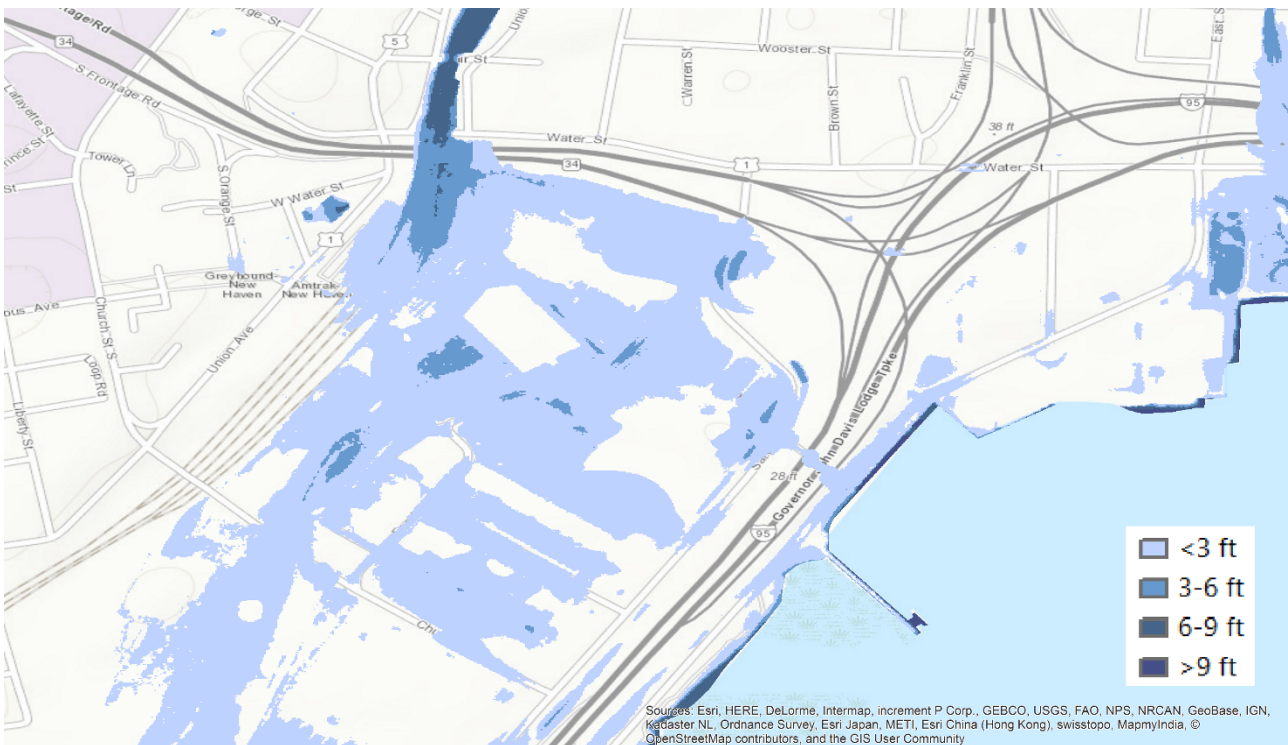


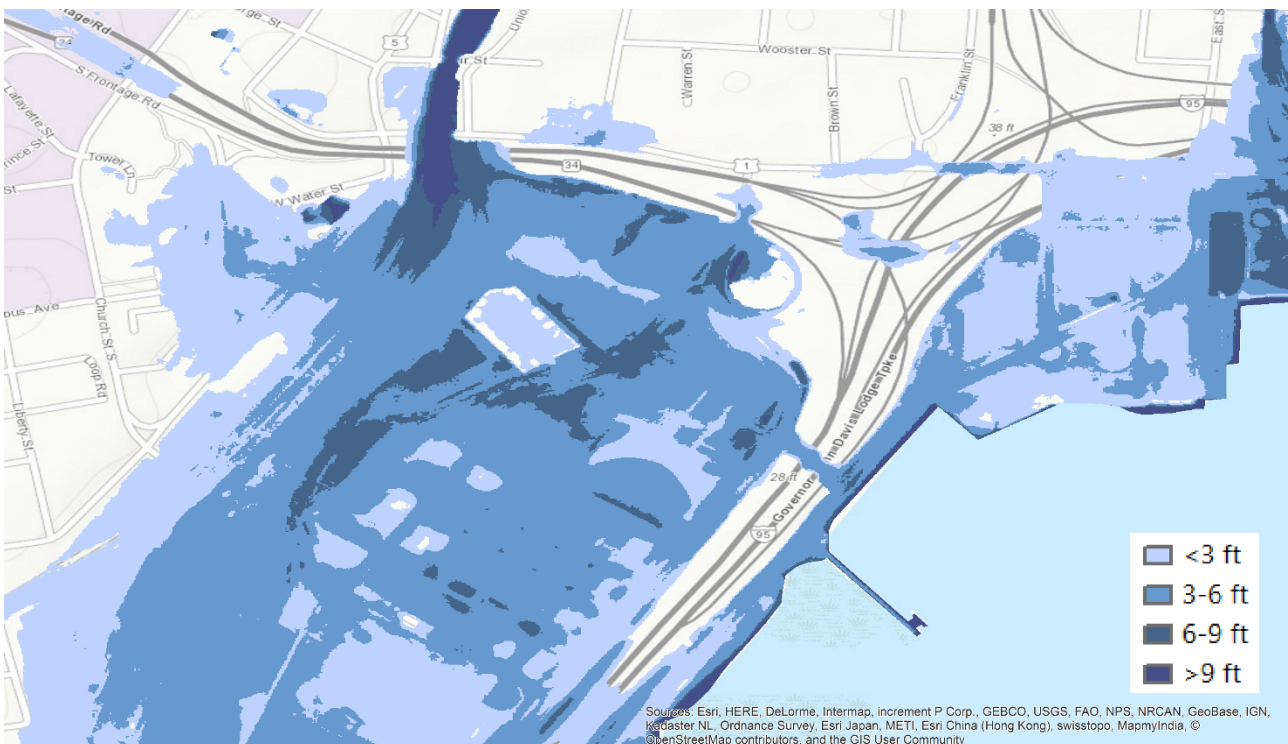
**Fig. 6.3** TWL for actual Superstorm Sandy flooding versus the simulation scenarios of future Sandy storm during low tide and high tide conditions



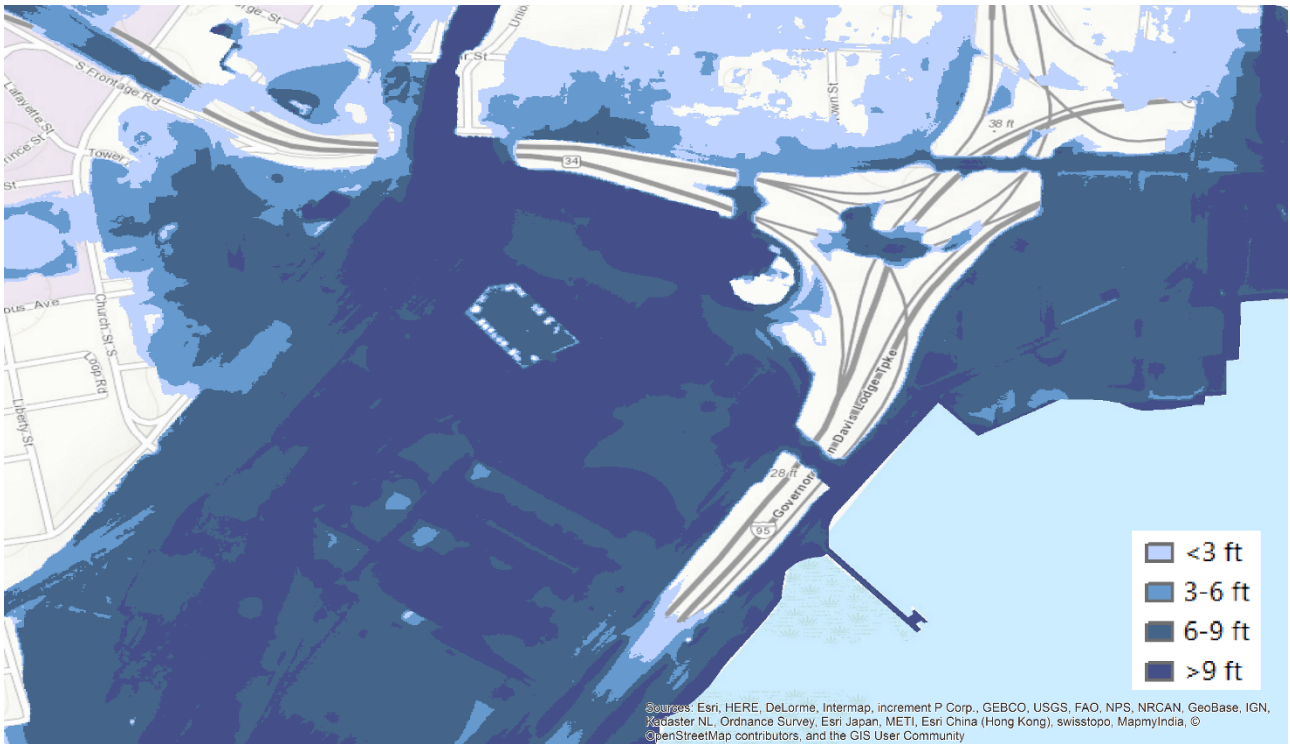
## Flood Maps



(a) Simulated flood map based on actual Superstorm Sandy water level data (Scenario 1)



(b) Simulated flood map scenario accounting for surge, simulated wave, inland flooding and sea level rise for future Superstorm Sandy during low tides (Scenario 2).



(c) Simulated flood map scenario accounting for surge, simulated wave, inland flooding and sea level rise for future Superstorm Sandy during high tides (Scenario 3).

**Fig. 6.4** Simulated flood maps for the three flooding scenarios described in Table 6.1








# CHAPTER 7 Start-of-the-art Resiliency Options

## 7.1 Introduction

In order to seek a better coastal protection option for the Long Wharf region, a review and understanding of current state-of-the-art resiliency options used in other U.S. coastal regions need to be carried out. Currently, some newly implemented resiliency options are concentrated along the eastern coast of United States and the coastal line of California, especially along the Atlantic coast of the northeastern United States, which is increasingly vulnerable to flooding due to the combined influence of storm surge, precipitation, wave, and sea level rise. This reality has brought on efforts to make greater use of different kinds of resiliency measures, which can be classified into three categories. In general, they are non-structural measures (also referred to as social measures), structural measures (also referred to as grey structures), and natural and nature-based measures (also referred to as green structures), respectively. Detailed subcategories of these three resiliency options are listed in Table 7.1.

**Table 7.1** Subcategories of three main resiliency options (Bridges et al. 2015)

NATURAL AND NATURE-BASED FEATURES AT A GLANCE				
				
<b>Dunes and Beaches</b>	<b>Vegetated Features (e.g., Marshes)</b>	<b>Oyster and Coral Reefs</b>	<b>Barrier Islands</b>	<b>Maritime Forests/Shrub Communities</b>
<b>Benefits/Processes</b> Breaking of offshore waves Attenuation of wave energy Slow inland water transfer	<b>Benefits/Processes</b> Breaking of offshore waves Attenuation of wave energy Slow inland water transfer Increased infiltration	<b>Benefits/Processes</b> Breaking of offshore waves Attenuation of wave energy Slow inland water transfer	<b>Benefits/Processes</b> Wave attenuation and/or dissipation Sediment stabilization	<b>Benefits/Processes</b> Wave attenuation and/or dissipation Shoreline erosion stabilization Soil retention
<b>Performance Factors</b> Berm height and width Beach slope Sediment grain size and supply Dune height, crest, and width Presence of vegetation	<b>Performance Factors</b> Marsh, wetland, or SAV elevation and continuity Vegetation type and density Spatial extent	<b>Performance Factors</b> Reef width, elevation, and roughness	<b>Performance Factors</b> Island elevation, length, and width Land cover Breach susceptibility Proximity to mainland shore	<b>Performance Factors</b> Vegetation height and density Forest dimension Sediment composition Platform elevation
General coastal risk reduction performance factors include: Storm surge and wave height/period, and water levels				

**Table 7.1** Subcategories of three main resiliency options (Cont'd) (Bridges et al. 2015)

NONSTRUCTURAL				STRUCTURAL				
Floodplain Policy and Management	Flood-proofing and Impact Reduction	Flood Warning and Preparedness	Relocation	Levees	Storm Surge Barriers	Seawalls and Revetments	Groins	Detached Breakwaters
<b>Benefits and Processes</b> Improved and controlled floodplain development Reduced opportunity for damages Improved natural coast environment	<b>Benefits and Processes</b> Reduced opportunity for damages Increased community resiliency No increase in flood potential elsewhere	<b>Benefits and Processes</b> Reduced opportunity for damages Increased community resiliency Improved public awareness and responsibility	<b>Benefits and Processes</b> Reduced opportunity for damages No increase in flood potential elsewhere Improved natural coast environment	<b>Benefits and Processes</b> Surge and wave attenuation and/or dissipation Reduced flooding Reduced risk for vulnerable areas	<b>Benefits and Processes</b> Surge and wave attenuation Reduced salinity intrusion	<b>Benefits and Processes</b> Reduced flooding Reduced wave overtopping Shoreline stabilization behind structure	<b>Benefits and Processes</b> Shoreline stabilization	<b>Benefits and Processes</b> Shoreline stabilization behind structure Wave attenuation
<b>Performance Factors</b> Wave height Water level Storm duration Agency collaboration	<b>Performance Factors</b> Wave height Water level Storm duration	<b>Performance Factors</b> Wave height Water level Storm duration	<b>Performance Factors</b> Wave height Water level Storm duration	<b>Performance Factors</b> Levee height, crest width, and slope Wave height and period Water level	<b>Performance Factors</b> Barrier height Wave height Wave period Water level	<b>Performance Factors</b> Wave height Wave period Water level Scour protection	<b>Performance Factors</b> Groin length, height, orientation, permeability, and spacing Depth at seaward end Wave height Water level Longshore transportation rates and distribution	<b>Performance Factors</b> Breakwater height and width Breakwater permeability, proximity to shoreline, orientation, and spacing
General coastal risk reduction performance factors include: Collaboration and shared responsibility framework, wave height, water level, and storm duration				General coastal risk reduction performance factors include: Storm surge and wave height/period, and water levels				

## 7.2 Resiliency options used in other U.S. coastal regions

The geographical distribution of current state-of-the-art resiliency options used in U.S. coastal regions is shown in Fig. 7.1. In total, there are 11 resiliency options that are currently used/proposed for those U.S. coastal regions (in green or orange color) and the descriptions of each resiliency option are presented in details herein.

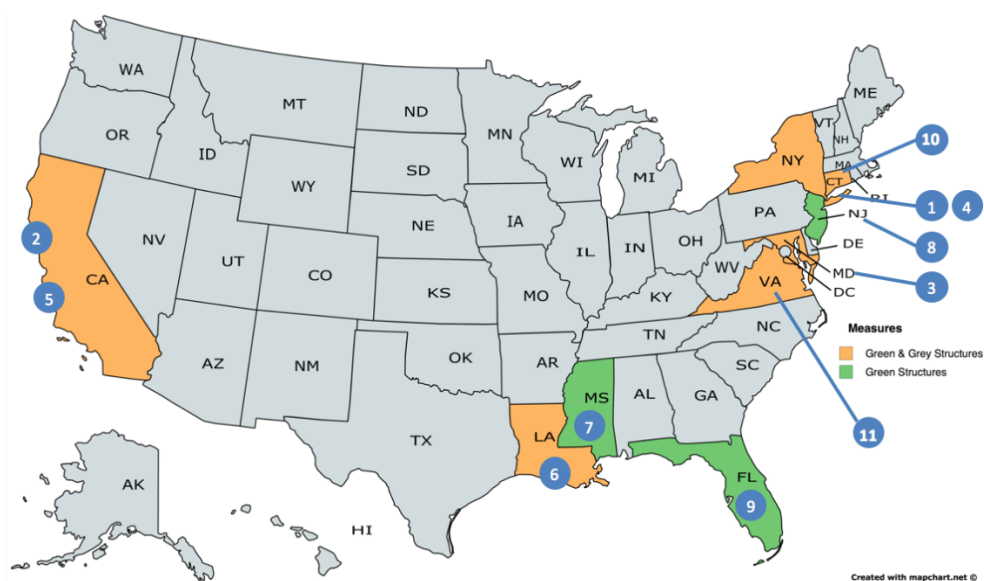


**Fig. 7.1** Resiliency options used in U.S. coastal regions

**Resiliency option #1:** Living shoreline to protect Shore Road on Long Island. (Hyman et al. 2014)  
As part of an FHWA research project, coastal engineers have analyzed the potential of implementing a living shoreline to protect the Shore Road in Brookhaven, New York, on the north shore of the Long Island. This road faced threat from inundation caused by the sea level rise. The living shoreline is implemented to increase the resiliency to wave damages and provide natural habitat for organisms. The construction of the living shoreline comprises a constructed marsh (e.g., saltmarsh and salt meadow) that parallels with the road, segmented groups of large boulders placed at the toe of seaward marsh with suitable geotextile fabric along the landward of them, and clean sand fill to establish a suitable marsh slope. The vegetation is transplanted from the nearby donor marshes. The existing revetment is buried by the fill to provide some redundant protection for the roadway.

**Resiliency option #2:** Living levee and breakwater to protect San Francisco Bay Bridge. (Metropolitan Transportation Commission 2014)

As part of an FHWA-funded pilot, the MTC and MPO for the San Francisco Bay Area conducted an analysis of installing a living levee in combination with a breakwater to protect the Bay Bridge touchdown from sea level rise, storm surge and waves. A living levee would protect against future inundation and flooding due to sea level rise and storm surges. A breakwater would reduce wave heights and protect the areas from future wave run-up, overtopping and wave-induced erosion along the shoreline that is expected to come with sea level rise. A result from an analysis using the design wave conditions and following the guidelines in the U.S. Army Corps of Engineers, Coastal Engineering Manual shows that the wave height can be reduced to at least half for the entire focus area behind the breakwater. The design also include freeboard to meet the requirement from FEMA accreditation, protect against wave overtopping, and be adaptable to accommodate higher sea level rise magnitudes. In case of higher sea level rise or wave height scenarios in the future, the current design elevation of the living levee and water breaker can be feasibly increased or can be constructed to a higher height.

In addition, the living shoreline used in the bay area has a flatter seaward slope than a traditional levee, which helps to dissipate more wave energy. This type of living shoreline can allow for the planting of vegetation, the creation of marsh habitat, the dissipation of wave energy, as well as the space to accommodate future adaptive management efforts that may be needed as sea levels continue to rise. The breakwater used in this area is separated into two parts. One is larger and is oriented perpendicular to the wave direction to reduce the wave height. The other is shorter and is oriented to minimize the effect of longshore sediment transport.

**Resiliency option #3:** Living shoreline projects in Maryland that protects the coastal road. (FHWA 2016, Maryland Department of Natural Resources 2016)

The Maryland Department of Natural Resources (DNR) worked on a living shoreline project together with the local landowners and public agencies to help install ecosystem-based living shorelines that can offer better protection than traditional hard structures without negative influence on the adjacent environment and properties. DNR was partnering with the Maryland State Highway Administration on installation of a living shoreline in order to protect the Hambrooks Boulevard in Cambridge, MD. The living shoreline uses vegetation and other natural resources to protect the shoreline from erosion while maintaining its dynamic nature and habitat features. The marsh grasses on the living shoreline provide shallow water habitat, a deep root system and dense foliage, which helps reduce wave action and hold soil in place.

In addition, Maryland has already standardized some criteria to determine the project type including structural and non-structural measures, materials to be used, e.g. sand, rock and etc., construction practices, and a general construction specification package. An assessment study of about 200

living shorelines in Maryland has shown the effectiveness of these projects on the maintenance of the coastal processes and reduction of erosion. These projects also demonstrate the ability of the living shoreline in attenuating wave forces, protecting the structures behind them, and maintaining sand and soils in place due to the vegetation root structure.

**Resiliency option #4:** Plumb Beach re-nourishment project. (USACE 2013)

This project is managed by the US Army Corps of Engineers to help reduce the coastal storm risk at the Plumb Beach and the Belt Parkway in Brooklyn, NY. This project is comprised of phase 1 and phase 2. Phase 1 involved placing approximately 127,000 cubic yards of sand in the severely eroded Plumb Beach area along the Belt Parkway. The sand was placed prior to the Superstorm Sandy and helped prevent severe damage to the Belt Parkway. Phase 1 also included a construction of a temporary geotube groin to mitigate the loss of the sands while the Corps awaited the approval of the Phase 2. Phase 2 involved the construction of two permanent stone groins at each end of the beach to help mitigate erosion in the long run. It also involved the construction of a permanent stone breakwater seaward parallel to the beach, where severe erosion occurred, to mitigate future sand loss. In addition, phase 2 also included planting vegetation on the sand dunes to strengthen them as well as installing sand fencing to trap the sand blowing landward.

To summarize, Phase 1 provides immediate mitigation and reduction benefits for coastal hazard. Phase 2 is designed to keep this benefit in place longer by managing the sand and reducing the need for future re-nourishment at the Plumb Beach area. In addition, this protects the natural resources in the area and provides the visitors access to the waterfront recreational resources.

**Resiliency option #5:** Beach nourishment to protect sections of California Highway 1. (Thornton et al. 2008)

The Association of Monterey Bay Area Governments developed a plan identifying four strategies to reduce coastal erosion along the southern Monterey Bay in California. One of these strategies involves beach nourishment to protect the critical infrastructure, including sections of California Highway 1. The beach nourishment measure is feasible in this region due to low wave energy, low sand transport, and the location is within a defined sub-cell, which means that the placed sand would remain at the site for a long period of time. Implementing beach nourishment at the southern bight provides substantial benefits for the recreational value of the shoreline and for the protection of its infrastructure assets. In addition, beach nourishment as a soft measure may reduce the need for the hard structures, and provide ecologic benefits associated with wider beaches.

Two different types of beach nourishment are adopted for this area, subaerial placement (on beach), and nearshore placement (in surf zone). Subaerial placement of sand is nourishment of the dry beach close to the water line, which results in an immediate artificially wide beach. Waves then redistribute the sand across the entire beach until equilibrium is reached. Through this process the dry beach will narrow from its initial nourished width to accommodate the profile adjustment. Nearshore placement nourishes the part of the littoral cell immediately seaward of the surf zone with intention that these sands can buffer the wave and meanwhile the waves can transport some of the sand onshore to make the beach wider. However, nearshore placement of sand widens the beach at a low rate than placing the same amount of sand directly on the beach. Some other potential erosion response alternatives are also listed in this project including hard structure approaches, dewatering, retention and bluff top development set back. However, hard structure approaches are not recommended in this region due to their ecological impacts.

**Resiliency option #6:** Protection for the Louisiana Highways LA-27, LA-82, and LA-182 in the Louisiana coastal master plan. (Louisiana CPRA 2007)

Louisiana's Coastal Protection and Restoration Authority developed a Coastal Master Plan to

provide a system-wide plan for reducing the hurricane flood risk and restoring land along the Louisiana coast. This plan outlines development of 109 coastal protection and restoration projects to be implemented over the next 50 years. The overall goal of this plan is to use a combination of restoration, nonstructural, and targeted structural measures to provide increased flood protection for all communities and use an integrated and synergistic approach to ensure a sustainable and resilient coastal landscape. Six of these projects are selected to create protective wetland buffers while considering the future climate impacts along several Louisiana highways, vulnerable to flooding from hurricanes, including LA-27, LA-82 and LA-182.

One of these projects involves hydrologic restoration, which repairs the degraded wetland by removing the blockages, including man-made levees and other built structures, to allow the natural flow of water. In the Mermentau Basin, three projects are implemented to increase the flow of freshwater to wetlands adjacent to LA-27 near Creole and sections of LA-82 near Grand Chenier and Pecan Island. Another project increases the connectivity among wetlands on either side of LA-182 in Chacahoula Basin. This project makes the connected wetlands more robust and provides a stronger natural barrier against shoreline erosion. The last project provides additional protection for LA-82 and includes two different parts. One is a marsh creation project which plans to establish a new wetland habitat near Grand Chenierand, and the other is a shoreline protection project which plans to construct rock breakwaters along the Schooner Bayou Canal near North Prong.

**Resiliency option #7:** Mississippi coastal improvements program (MsCIP). (USACE 2009, USACE 2014)

The purpose and scope of this program is to conduct an analysis and design for comprehensive improvements and modifications to the existing protective measures in the coastal region of Mississippi. The interest of this program includes damage reduction from storms and hurricanes, ecosystem restoration for preservation of fish, wildlife and habitat functions and values, prevention of saltwater intrusion, prevention of coastline erosion, and other related water resource purpose.

A relatively small set of alternatives are studied and analyzed in Phase 1. Other comprehensive measures and alternatives identified in this program are to be included in Phase 2 and Phase 3 study efforts to be accomplished during the next 30 to 40 years. The final plans in Phase 1 include:

- Turkey Creek ecosystem restoration of 689 Acres south of the railroad and maintained by burning.
- Bayou Cumbest ecosystem restoration of 110 acres by excavating filled in areas, removing exotic species, planting native species at a 1-meter density, filling in ditches, and acquisition of properties.
- Dantzler ecosystem restoration of 385 acres and maintained by burning.
- Admiral Island ecosystem restoration of 123 acres by excavating filled in areas, removing exotic species, planting native species at a 1-meter density, filling in ditches, and acquisition of properties.
- Franklin Creek ecosystem restoration of 149 acres north and south of the railroad and maintained by burning.
- A submerged aquatic vegetation restoration pilot study in Bayou Cumbest before implementing it in a large scale.
- Coast-wide beach and dune restoration with construction of a 2' high 60' wide dune through the existing berm expansion, and placing sand fencing and plantings.

- Deer Island restoration of 128 acres of emergent tidal marsh habitat, 78 acres of coastal maritime forest, 86 acres of beach habitat, 30 acres of dune habitat and extension of both existing breakwater.
- Barrier Island restoration including the restoration of Ship Island, littoral zone sand additions at the east ends of Petit Bois and East Ship Island, changes in maintenance dredging practices and a study to define the best restoration option for Cat Island.
- Forrest Height hurricane and storm damage reduction with construction of a levee at an elevation of 21 feet with clearing and snagging of channel.
- High hazard area risk reduction plan that provides immediate buyout opportunities for the most high risk areas and relocates those structures.
- Waveland flood proofing that construct a pilot project involving new methods for elevating structures in the hardest hit areas of Waveland using FEMA's new 550 guidelines.
- Freshwater diversion from the Mississippi River to the Mississippi Sound to provide sufficient inflow to support oyster reef health and productivity in coastal Mississippi.

**Resiliency option #8:** Enhancing and managing risk to the New Jersey coastal natural and nature-based features. (Simm et al. 2015)

The U.S. Army ERDC; USACE District, Philadelphia; Forsythe National Wildlife Refuge (NWR); and HR Wallingford (HRW) among others including USGS are working on a variety of projects designed to improve the resiliency of the New Jersey coastline by enhancing and managing risk to existing natural and nature-based features using a systems approach.

The program comprises of three independent projects. The first one is management of navigation channels and sediments along the New Jersey Intracoastal Waterway. ERDC and USACE Philadelphia District examined placement options for the required dredging of the New Jersey Intracoastal Waterway that would enhance existing natural and nature-based features near the navigation channel. The second one is ecosystem restoration and enhancement in response to relative sea level rise at the Forsythe National Wildlife Refuge. ERDC and Forsythe NWR are planning a variety of ecosystem restoration and enhancement projects intended to increase the resiliency of the refuge's ecological resources, including restoring and enhancing salt marshes and impoundments and developing long-term plans for monitoring and adaptation in response to future disasters, sea level change, and anthropogenic changes in the system. The last one is sea level change vulnerability and adaptation measures for barrier coasts. A barrier island evaluation method was completed to predict the erosion and overtopping response of dune-beach systems to sea level change using Long Beach Island, NJ. The methodology can be used to examine the impacts of proposed policy decisions for managing barrier island and Back Bay systems on submergence and increasing flood risk over time.

**Resiliency option #9:** Regional sediment management in northeast Florida. (Simm et al. 2015)

Net sediment transport is from north to south in this region, although there are reversals downdrift of the coastal inlets as well as complex interactions between the inlets, river systems, estuaries, and waterways. As a result of these complex sediment transport patterns, beaches downdrift of coastal inlets have eroded; sand is needed on beaches to create dunes and berms; and, fine sediments are needed in estuaries and bays for habitat creation. The systems approach has been largely realized by connecting dredging activities at the Federal and Navy navigation channels with the coastal storm risk management and natural and nature-based needs of the adjacent beaches, estuaries, and bays. The USACE Jacksonville District has coordinated the dredging and placement activities, reduced costs, and increased the coastal resiliency of the region.



**Resiliency option #10:** Innovative living shoreline construction at Stratford Point, CT. (Sacred Heart University 2014)

November 8, 2013 – Connecticut Audubon Society and Sacred Heart University have been awarded a \$59,000 Long Island Sound Futures Fund grant to construct an innovative “living shoreline” at Stratford Point, to improve critical bird and wildlife habitat and protect the State’s coastline from storms like Superstorm Sandy.

The living shoreline includes the construction of a reef consisting of 40 permeable concrete reef balls—a technology never before used in Long Island Sound—along with the restoration of a salt marsh behind the reef. This project is constructed in roughly 3.5 acres of intertidal zone at the 40-acre coastal estuary restoration site at Stratford Point, which is managed by Connecticut Audubon Society (CAS). One of the goals of this project is to test the feasibility of the living shoreline that could be adopted by other coastal communities for resiliency protection against hurricanes and storms, and for preventing erosion and other impacts caused by sea level rise. The living shoreline works by slowing down and breaking up waves and storm surges that cause erosion, allowing for sediment deposition and for protective tidal marsh plants to take root. It will also help protect the newly restored upland coastal habitats that CAS and Sacred Heart have undertaken at Stratford Point over the past four years. This project also greatly improves its value as a key bird and fish habitat in the heart of the Housatonic River estuary.

**Resiliency option #11:** Virginia resilient project. (SAGE 2016)

In Norfolk, a segmented stone sill was built at the marsh toe and volunteers planted marsh vegetation behind it. The pavement was also replaced with an elevated boardwalk, and shell was placed in shaded area to control erosion.

In Hampton, 5500 square feet of tidal wetlands and approximately 1600 plugs of saltmarsh cordgrass and other native plants are used. Debris removal, native grass plantings, small stone breakwater are also included in this project.

### **7.3. FHWA climate resiliency pilot program**

In 2013-2015, FHWA worked with State Departments of Transportation (DOTs) and metropolitan planning organizations (MPOs) to undertake nineteen pilot projects from across the country to assess the transportation vulnerability to climate change and extreme weather events and evaluate adaptation options for improving resiliency of their transportation systems (FHWA 2016). The locations of these nineteen newly implemented pilot projects together with those five previous pilot projects carried out in 2010-2011 are shown in Fig. 7.2.

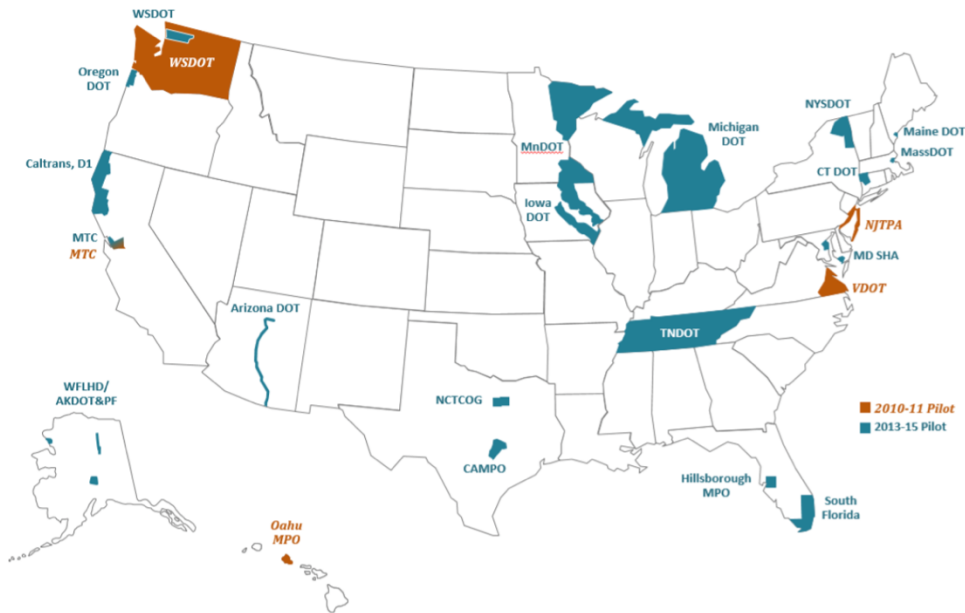


**Fig. 7.2** 2010-2011 and 2013-2015 pilot study areas. (FHWA 2016)

Each of the nineteen pilot projects took unique approaches to conduct vulnerability assessments and evaluate adaptation options with the FHWA’s Climate Change and Extreme Weather Vulnerability Assessment Framework as a reference. The 2013-2015 pilot projects continued to utilize this framework and identify lessons learned from vulnerability assessments and evaluation of adaption options. The methods and findings reflect locally-specific transportation properties and corresponding climate conditions.

Several of these pilot projects carried out along the coastline focus on improving the resiliency of structures to extreme weather events including storm surge, flood, and sea level rise caused by climate change, e.g., the project carried out by Hillsborough MPO in Florida and the project carried out by Maine DOT. The project conducted by CTDOT focuses on assessing the system-level vulnerability of bridge and culvert structures from inland flooding associated with extreme precipitation events that have been observed at an increasing rate in recent years and result in more damage to infrastructures. This project helped develop information on vulnerability that can be used to assist CTDOT in identifying replacement and reconstruction efforts where needed and conduct assessments for facilities and assets in a part of the state that have not ever been comprehensively studied. Additionally, this project also complements previous assessments of coastal assets and adaptation options conducted by CTDOT, both independently and collectively, with other state agencies including the tri-state Superstorm Sandy follow-up and vulnerability assessment and adaption analysis.

#### **7.4. Resiliency options for Long Wharf, New Haven, CT**

After investigating each of the current state-of-the-art resiliency options conducted by different coastal state agencies, it appears that the most popular and reliable resiliency option is the combination of structural measures and natural and nature-based features. With regard to the Long Wharf region, the resiliency option of combining living shorelines and breakwaters may be appropriate.

Living shorelines are essentially tidal wetlands constructed along a shoreline to reduce costal erosion, maintain dynamic shoreline processes, and provide habitat for organisms. In addition, the

living shorelines can also provide waterfront recreation. Several studies show that the living shorelines can eliminate the wave damage from high tide. One laboratory investigation shows that *Spartina Alterniflora* marshes are effective at reducing the wave height by as much as 90% over a distance of 30 ft. through the marsh and hence is considered as an effective way to protect the coastline from wave damage. Although the living shoreline itself cannot prevent flooding damage when the water levels are above the roadway elevation, some studies show that saltmarshes are at least keeping pace with the present-day rate of sea level rise in the Long Island area. In addition, the constructability of the living shoreline could be easily accomplished by a coastal marine contractor with restoration experience. The cost of establishing a living shoreline is less than the traditional method using hard structures (gray structures). Some initial adaptive management strategies need to be applied, such as provide supplemental plantings during first several growing seasons to build the living shoreline. Overall, the living shoreline may protect the Long Wharf area that is already low-lying; and, vulnerable to storm surge and sea level rise as well as preserve the natural aesthetics of the shoreline.

Breakwater is the other important facet of this combinative resiliency strategy. Breakwaters are constructed with large pieces of rock or small rubble. They are usually deployed offshore and parallel to the shoreline to serve as protection from wave energy that would impact the living shoreline and cause erosion and damage or removal of the tidal plants. Numerous studies have already been conducted to numerically or experimentally investigate the effects of breakwaters on the wave property and damage to the structures behind it after the wave passing or overtopping the breakwater. All of these studies show that breakwaters, as a protective measure off the shoreline, can result in a significant reduction for the wave height and wave run-up on the structures standing behind. In addition, if a living shoreline is installed without a breakwater, it would most likely be eroded and damaged by wave attack. The breakwater may help reduce the wave energy, preserve the shoreline integrity, and prevent degradation of living shorelines adjacent to the coast at Long Wharf. Therefore, the living shoreline and breakwater, together, may offer all of the benefits of protection from inundation, wave overtopping, wave-induced erosion, and enhancement of the living shoreline.

However, in the past several years, breakwaters have not always behaved as intended during some hurricane events.. Those breakwaters could not provide sufficient protection of the shoreline as stated in researched literature, including significant wave run-up reduction and wave attenuation. Some were even destroyed during the hurricane events. One example is that of the three breakwaters protecting the Los Angeles-Beach Harbor. The breakwaters suffered damage and lost their protective functionality during the heavy wave event generated by the winds from Hurricane Marie. The middle breakwater suffered the most significant damage with several breaches and wave overtopping, and hence the breakwater allowed greater transmission of wave energy into the inner portions of the harbor. The investigation after the Hurricane Marie event shows that those three breakwaters, in their current condition, remain functional but compromised. With future heavy wave and storm surge events in this area, their functionality will continuously decrease. Besides this, there exist numerous examples where protection failures of breakwaters have caused severe flooding damage to the coastal areas.

The inconsistency between the breakwater behavior in reality and that stated in the literature might be because of the fact that both the numerical and experimental models used to simulate the wave interaction with breakwaters generally only consider 2D effect. In fact, the maximum wave height or wave energy transmitted behind the breakwater might be caused by the diffraction of wave and the incident angle of wave with respect to the orientation of the breakwater. Meanwhile, for multiple types of offshore breakwater, the wave behavior behind breakwaters will be more complicated and the length of gap between each breakwater will have a more pronounced effect on

the performance of breakwaters. Hence, a numerical study considering the 3D effect might be necessary to investigate the real effect of breakwaters on wave attenuation behind it.

Another important factor that influences the behavior of breakwaters is the rise in the sea level. Since the sea level keeps increasing, the breakwaters built under current design criteria might not be suitable in the future. Similarly, severe climate events might also degrade the performance of breakwaters. The breakwater is functional as long as wave condition is average, but a significant wave or storm will compromise its functionality. Therefore, a sensitivity study for the behavior of breakwaters with respect to the sea level rise might also be necessary to be carried out.

Above all, a numerical study used to simulate the 3D effect of breakwaters is essential for the breakwater design at any specific location. This kind of study can investigate the behavior of breakwaters with different design parameters and under different scenarios. It can also provide insight about how to improve the performance of breakwaters for wave attenuation in the future by considering the layout, design parameters, and shape etc.

## **Concluding Remarks**

In the present study, the potential water level is estimated using a simulation scheme that combines a high-resolution atmospheric model, a land-surface model, and a parametric wind-wave model considering both the actual Superstorm Sandy conditions and simulations of future climate Superstorm Sandy scenarios. Based upon these derived total water levels combining surge, wave and precipitation flooding effects, GIS-based flood inundation maps were generated using high resolution DEM information of the study area. The major finding from this resiliency study is that the area is highly vulnerable to hurricane events, particularly possible future storms that could potentially overlap with high tide conditions. Specifically, the simulated future Superstorm Sandy scenarios showed enhanced vulnerability of the road network and much larger inundation areas than the ones that occurred during Superstorm Sandy.

Evaluation of resiliency options throughout the nation was conducted to provide potential options for this study area, which are summarized below:

- A combination of living shorelines and breakwaters for this region;
- Combination of river flooding and 3D effects of breakwater studies, including experimental validations; and,
- Climate and sea level rise may significantly affect the performance of these resiliency options and should be considered in future studies.

## Bibliography

- Battjes, J. A. (1974). "Surf similarity." *Proceedings of the 14th international conference on coastal engineering, ASCE*, 1(14), 466–480.
- Batts, M. E., Simiu, E., and Russell, L. R. (1980). "Hurricane wind speeds in the United States." *Journal of the Structural Division*, 106(10), 2001–2016.
- Bouws, E., Günther, H., Rosenthal, W., and Vincent, C. L. (1985). "Similarity of the wind wave spectrum in finite depth water: 1. Spectral form." *J. Geophys. Res.*, 90(C1), 975–986.
- Bridges, T. S., Wagner, P. W., Burks-Copes, K. A., Bates, M. E., Collier, Z. A., Fischelich, C. J., ... & Russo, E. J. (2015). *Use of natural and nature-based features (NNBF) for coastal resiliency*. Engineer Research and Development Center, Vicksburg MS Environmental Lab: Vicksburg, MS
- Carter, D. J. T., and Challenor, P. G. (1981). "Estimating return values of environmental parameters." *Journal of the Royal Meteorological Society*, 107(1), 259–266.
- City of New Haven. (2015). *New Haven Vision 2025: A Plan for a Sustainable, Healthy, and Vibrant City*. New Haven, Connecticut
- Davison, A. C., and Smith, R. L. (1990). "Models for exceedances over high thresholds." *Journal of the Royal Statistical Society. Series B (Methodological)*, 52(3), 393–442.
- Dee, D. P., Uppala, S. M., Simmons, A. J., Berrisford, P., Poli, P., Kobayashi, S., ... Vitart, F. (2011). The ERA-Interim reanalysis: configuration and performance of the data assimilation system. *Quarterly Journal of the Royal Meteorological Society*, 137(656), 553–597. <http://doi.org/10.1002/qj.828>
- Department of the Environment and Water Resources. (2007). *An assessment of the need to adapt buildings for the unavoidable consequences of climate change*.
- Elsner, J. B., Kossin, J. P., and Jagger, T. H. (2008). "The increasing intensity of the strongest tropical cyclones." *Nature*, 455(7209), 92–95.
- Federal Highway Administration. (2016). *2013-2015 Climate Resiliency Pilot Program: Outcomes, Lessons Learned, and Recommendations*. Retrieved from [https://www.fhwa.dot.gov/environment/sustainability/resiliency/pilots/2013-2015\\_pilots/final\\_report/fhwahep16079.pdf](https://www.fhwa.dot.gov/environment/sustainability/resiliency/pilots/2013-2015_pilots/final_report/fhwahep16079.pdf)
- Federal Highway Administration. (2016). *Green Infrastructure Techniques for Improving Coastal Highway Resiliency*. Retrieved from [https://www.fhwa.dot.gov/environment/climate\\_change/adaptation/ongoing\\_and\\_current\\_research/green\\_infrastructure/](https://www.fhwa.dot.gov/environment/climate_change/adaptation/ongoing_and_current_research/green_infrastructure/)
- Maryland Department of Natural Resources. (2016). *Maryland Coastal Resiliency Assessment*. Retrieved from [http://dnr2.maryland.gov/ccs/Documents/MARCH-2016\\_MDCoastalResiliencyAssessment.pdf](http://dnr2.maryland.gov/ccs/Documents/MARCH-2016_MDCoastalResiliencyAssessment.pdf)
- Meehl, G. A., Covey, C., Delworth, T., Latif, M., McAvaney, B., Mitchell, J. F. B., ... Taylor, K. E. (2007). The WCRP CMIP3 multimodel dataset: A new era in climatic change research. *Bulletin of the American Meteorological Society*. <http://doi.org/10.1175/BAMS-88-9-1383>
- Metropolitan Transportation Commission. (2014). *Climate Change and Extreme Weather Adaptation Options for Transportation Assets in the Bay Area: Pilot Project*. Retrieved from [http://mtc.ca.gov/sites/default/files/MTC\\_ClimateChng\\_ExtmWthr\\_Adtpn\\_Report\\_Final.pdf](http://mtc.ca.gov/sites/default/files/MTC_ClimateChng_ExtmWthr_Adtpn_Report_Final.pdf)
- Guedes Soares, C., and Scotto, M. (2001). "Modelling uncertainty in long-term predictions of significant wave height." *Ocean Engineering*, 28(3), 329–342.
- Guedes Soares, C., and Scotto, M. G. (2004). "Application of the r largest-order statistics for long-term predictions of significant wave height." *Coastal Engineering*, 51(5–6), 387–394.

- Hasselmann, K., Barnett, T. P., Bouws, E., Carlson, H., Cartwright, D. E., Enke, K., Ewing, J. A., Gienapp, H. Hasselmann, D.E. Kruseman, P., Meerburg, A., Müller, P., Olbers, D. J., Richter, K., Sell, W., and Walden, H. (1973). *Measurements of wind-wave growth and swell decay during the JOint North Sea Wave Project (JONSWAP)*. *Deutsches Hydrographisches Institut*.
- Hedges, T. S., and Mase, H. (2004). "Modified Hunt's equation incorporating wave setup." *Journal of Waterway, Port, Coastal, and Ocean Engineering*, 130(3), 109–113.
- Hedges, T. S., and Reis, M. T. (1998). "Random wave overtopping of simple sea walls: A new regression model." *Proceedings of the Institution of Civil Engineers: Water and Maritime Engineering*, 130(1), 1–10.
- Hu, K., and Chen, Q. (2011). "Directional spectra of hurricane-generated waves in the Gulf of Mexico." *Geophysical Research Letters*, 38(19), L19608.
- Hyman, R., Kafalenos, R., Beucler, B., & Culp, M. (2014). *Assessment of Key Gaps in the Integration of Climate Change Considerations into Transportation Engineering: Task 2.3 (No. FHWA-HEP-15-059)*, Fairfax, VA
- IPCC. (2007). *Change, Intergovernmental Panel On Climate. Climate Change 2007: The physical science basis, summary for policy makers. Agenda 6.07, 2007: 333. Contribution of working group I to the fourth assessment report of the intergovernmental panel on climate change. Intergovernmental Panel on Climate Change.*
- Kikkawa, H., Shiigaki, H., and Kono, T. (1968). "Fundamental study of wave over-topping on levees." *Coastal Engineering in Japan*, 11, 107–115.
- Knutson, T. R., McBride, J. L., Chan, J., Emanuel, K., Holland, G., Landsea, C., Held, I., Kossin, J. P., Srivastava, a K., and Sugi, M. (2010). "Tropical cyclones and climate change." *Nature Geoscience*, 3, 157–163.
- Kobayashi, N., and Karjadi, E. A. (1994). "Surf-similarity parameter for breaking solitary-wave runup." *Journal of Waterway, Port, Coastal, and Ocean Engineering (ASCE)*, 120(6), 645–650.
- Lackmann GM (2015) "Hurricane Sandy before 1900, and after 2100". *Bulletin of the American Meteorological Society* 96:547-560
- Li, Q., Wang, C., and Zhang, H. (2016). "A probabilistic framework for hurricane damage assessment considering non-stationarity and correlation in hurricane actions." *Structural Safety*, 59, 108–117.
- Lin, I.-I., Pun, I.-F., and Wu, C.-C. (2008). "Upper-ocean thermal structure and the western north pacific category 5 typhoons. Part II: dependence on translation speed." *Monthly Weather Review*, 136(9), 3288–3306.
- Louisiana CPRA. (2007). *Louisiana's Comprehensive Master Plan for a Sustainable Coast*. Retrieved from <http://coastal.la.gov/a-common-vision/2012-coastal-master-plan/>
- Madsen, P. A., and Fuhrman, D. R. (2008). "Run-up of tsunamis and long waves in terms of surf-similarity." *Coastal Engineering*, 55(3), 209–223.
- Madsen, P. a., and Schäffer, H. a. (2010). "Analytical solutions for tsunami runup on a plane beach: single waves, N-waves and transient waves." *Journal of Fluid Mechanics*, 645(2010), 27.
- Metropolitan Transportation Commission. (2014). *Climate Change and Extreme Weather Adaptation Options for Transportation Assets in the Bay Area: Pilot Project*. Retrieved from [http://mtc.ca.gov/sites/default/files/MTC\\_ClimateChng\\_ExtremWthr\\_Adtpn\\_Report\\_Final.pdf](http://mtc.ca.gov/sites/default/files/MTC_ClimateChng_ExtremWthr_Adtpn_Report_Final.pdf)
- van der Meer, J. W. (2002). "Technical report wave run-up and wave overtopping at dikes." *Technical Advisory Committee on Flood Defence, Delft, The Netherlands*, 43.
- van der Meer, J. W., and Janssen, J. P. F. M. (1995). "Wave run-up and wave overtopping at dikes." *Wave forces on inclined and vertical wall structures*, N. Kobayashi and Z. Demirbilek, eds., ASCE, New York, 1–27.



- Mei, W., Pasquero, C., and Primeau, F. (2012). "The effect of translation speed upon the intensity of tropical cyclones over the tropical ocean." *Geophysical Research Letters*, 39(7), 1–6.
- Minimum Design Loads for Buildings and Other Structures, ASCE 7-10*. (2013). American Society of Civil Engineers, Reston, Virginia 20191.
- New Haven City Plan Department. (2011). *City of New Haven natural hazard mitigation plan update*. City of New Haven, City of New Haven.
- Owen, M. W. (1980). *Design of seawalls allowing for wave overtopping*. Report Ex924, Wallingford, U.K.
- Peterka, J. A., and Shahid, S. (1998). "Design gust wind speeds in the United States." *Journal of Structural Engineering*, 124(2), 207–214.
- Pullen, T., Allsop, N. W. H., Bruce, T., Kortenhuis, A. Schuttrumpf, H., and van der Meer, J. W. (2007). *EurOtop—Wave overtopping of sea defences and related structures: Assessment manual*.
- Reis, M. T., Hu, K., Hedges, T. S., and Mase, H. (2008). "A Comparison of empirical, semiempirical, and numerical wave overtopping models." *Journal of Coastal Research*, 24(2A), 250–262.
- Sacred Heart University. (2014). *Unique Installation to Be Completed as Part of Stratford Point Restoration Project [Press Release]*. Retrieved from <http://www.sacredheart.edu/aboutshu/news/newsstories/2014/may/unique-installation-to-be-completed-as-part-of-stratford-point-restoration-project.html>
- Simiu, E., Vickery, P., and Kareem, A. (2007). "Relationship between Saffir-Simpson hurricane scale wind speeds and peak 3- sec gust speeds over open terrain." *Journal of Structural Engineering*, 133(7), 1043–1045.
- Simm, J. D., Guise, A., Robbins, D., & Engle, J. (2015). *US North Atlantic Coast Comprehensive Study: Resilient Adaptation to Increasing Risk*. Retrieved from [http://www.nad.usace.army.mil/Portals/40/docs/NACCS/NACCS\\_main\\_report.pdf](http://www.nad.usace.army.mil/Portals/40/docs/NACCS/NACCS_main_report.pdf)
- Skamarock, W. C. et al. (2008) A Description of the Advanced Research WRF Version 3 TN–475+STR
- Sobey, R. J., and Orloff, L. S. (1995). "Triple annual maximum series in wave climate analyses." *Coastal Engineering*, 26(3–4), 135–151.
- Stewart, M. G., Rosowsky, D. V, and Huang, Z. (2003). "Hurricane risks and economic viability of strengthened construction." *Natural Hazards Review*, 4(1), 12–19.
- Systems Approach to Geomorphic Engineering (SAGE). (2016). *Resiliency Project database*. Retrieved from <http://sagecoast.org/info/searchresults.php>
- The overseas coastal area development institute of Japan (OCDI). (2007). *Technical standards and commentaries for port and harbour facilities in Japan*. OC DI, Tokyo (in Japanese).
- Thomas, T. J., and Dwarakish, G. S. (2015). "Numerical wave modelling – A review." *Aquatic Procedia*, 4, 443–448.
- Thornton, E., Dugan, J., & Griggs, G. (2008). *Coastal Regional Sediment Management Plan for Southern Monterey Bay*. San Francisco, CA
- U.S. Army Corps of Engineers (USACE). (2002). *Coastal engineering manual*. EM 1110-2-1100, USACE, Washington, DC.
- U.S. Army Corps of Engineers. (2009). *Comprehensive plan and integrated programmatic environmental impact statement, Mississippi Coastal Improvements Program (MsCIP) Hancock, Harrison, and Jackson Counties, Mississippi: Mobile, Ala., Army Engineer District, v. 1, 417 p.*
- U.S. Army Corps of Engineers. (2013). *Army Corps awards \$2 million contract for Phase II of Plumb Beach coastal storm risk reduction work in Brooklyn*. Retrieved from

<http://www.nad.usace.army.mil/Media/News-Releases/Article/483846/army-corps-awards-2-million-contract-for-phase-ii-of-plumb-beach-coastal-storm/>

- U.S. Army Corps of Engineers. (2014). *Mississippi Coastal Improvements Program (MsCIP) comprehensive barrier island restoration Hancock, Harrison, and Jackson Counties, Mississippi, Draft supplemental environmental impact statement: Mobile, Ala., Army Engineer District*, 282 p.
- Valamanesh, V., Myers, A. T., and Arwade, S. R. (2015). "Multivariate analysis of extreme metocean conditions for offshore wind turbines." *Structural Safety*, Elsevier Ltd, 55, 60–69.
- Valamanesh, V., Myers, A. T., Arwade, S. R., Hajjar, J. F., Hines, E., and Pang, W. (2016). "Wind-wave prediction equations for probabilistic offshore hurricane hazard analysis." *Natural Hazards*, Springer Netherlands, 83(1), 541–562.
- Vickery, P. J., Skerlj, P. F., and Twisdale, L. A. (2000). "Simulation of hurricane risk in the U.S. using empirical track model." *Journal of Structural Engineering*, 126(10), 1222–1237.
- de Waal, J. P., and van der Meer, J. W. (1992). "Wave runup and overtopping on coastal structures." *Coastal Engineering Proceedings*, 1(23), 1758–1771.
- Wolf, J. (2009). "Coastal flooding: Impacts of coupled wave-surge-tide models." *Natural Hazards*, 49(2), 241–260.
- Young, I. R. (1988). "Parametric hurricane wave prediction model." *Journal of Waterway Port Coastal and Ocean Engineering*, 114(5), 637–652.
- Young, I. R. (2003). "A review of the sea state generated by hurricanes." *Marine Structures*, 16(3), 201–218.
- Young, I. R. (2006). "Directional spectra of hurricane wind waves." *Journal of Geophysical Research: Oceans*, 111(8), C08020.
- Young, I. R., and Vinoth, J. (2013). "An 'extended fetch' model for the spatial distribution of tropical cyclone wind-waves as observed by altimeter." *Ocean Engineering*, Elsevier, 70, 14–24.
- Zhu, J. and Zhang, W. (2017). "Numerical Simulation of Wind and Wave Fields for Coastal Slender Bridges." *ASCE Journal of Bridge Engineering*, (22)3, 04016125, 10.1061/(ASCE)BE.1943-5592.0001002